MASSACHUSETTS INSTITUTE OF TECHNOLOGY
LINCOLN LABORATORY

ACCURACY LIMITATIONS OF HYPERBOLIC MULTILATERATION SYSTEMS

H. B. LEE

TECHNICAL NOTE 1973-11

22 MAR 1973

LEXINGTON MASSACHUSETTS

TECHNICAL REPORT STANDARD TITLE PAGE

1. Report No.	2. Government Accession No.	3. Recipient's Catalog No.
DOT/TSC-241-3		

4. Title and Subtitle	5. Report Date
Accuracy Limitations of Hyperbolic Multilateration Systems	22 March 1973
	6. Performing Organization Code
7. Author(s)	8. Performing Organization Report No.
Harry B. Lee	Technical Note 1973-11
9. Performing Organization Name and Address Massachusetts Institute of Technology Lincoln Laboratory P.O. Box 73 Lexington, Massachusetts 02173	10. Work Unit No. 11. Contract or Grant No. DOT-TSC-241
12. Sponsoring Agency Name and Address Transportation Systems Center Department of Transportation Cambridge, Massachusetts	13. Type of Report and Period Covered Technical Note 14. Sponsoring Agency Code

15. Supplementary Notes

The work reported in this document was performed at Lincoln Laboratory, a center for research operated by Massachusetts Institute of Technology.

16. Abstract

This report is an analysis of the accuracy limitations of hyperbolic multilateration systems. A central result is a demonstration that the inverse of the covariance matrix for positional errors corresponds to the moment of inertia matrix of a simple mass configuration. The insight afforded by this fact is used to resolve a number of questions relating to accuracy. Specific questions addressed include the following.

1. How does accuracy depend upon the number of receivers?
2. How does accuracy depend upon the deployment of receivers?
3. What is the maximum accuracy that can be obtained from N receivers? How should the receivers be deployed to maximize accuracy?
4. How do altitude errors compare to horizontal errors in satellite based systems? In ground based systems?
5. How is accuracy impacted by dropout of any particular receiver?

17. Key Words	18. Distribution Statement
aircraft surveillance position determination least squares estimation multilateration geometric dilution of precision navigation hyperbolation	Availability is unlimited. Document may be released to the National Technical Information Service, Springfield, Virginia 22151, for sale to the public.

19. Security Classif. (of this report)	20. Security Classif. (of this page)	21. No. of Pages	22. Price
Unclassified	Unclassified	118	

Form DOT F 1700.7 (8-69)

CONTENTS

		Page
I.	Introduction	1
II.	Summary of Results	4
III.	Equations for Accuracy Measures	7
IV.	Inverse of the Error Magnification Matrix	15
V.	Calculation of the Error Magnification Matrix Γ	20
VI.	Approximate Calculation of Γ	30
VII.	Dependence of Accuracy on the Number of Beacons	44
VIII.	Dependence of Accuracy on Cone Angle	47
IX.	Dependence of Accuracy on Direction	52
X.	Error Minimization I	57
XI.	Error Minimization II	63
XII.	Sensitivity of Accuracy to Single Beacon Dropout	84
XIII.	Ground Based Multilateration Systems	89
XIV.	The Effect on Accuracy of Correlated Noise	93
XV.	Independent Altitude Measurement	98
XVI.	References	102

APPENDICES

		Page
I.	Proof that $r_{ii} \geq 1/L_{ii}$.	103
II.	Proof that $\overline{Y^2} \leq (1 - \overline{Y^T})(\overline{Y^T} - \cos \phi)$.	106
III.	Proof of Inequalities (9.4) and (9.7).	108
IV.	Interpretation of Error Minimization Steps in Example 11.3.	111

I. INTRODUCTION

This report examines a variety of issues related to the accuracy of hyperbolic multilateration systems.

The distinguishing feature of hyperbolic multilateration systems is that position is estimated from differential arrival times of a pulse transmitted over several distinct paths. Thus no absolute time reference is required.

Hyperbolic multilateration systems can take many different forms. Figure 1.1 depicts an example of a system that could be utilized for aircraft surveillance. The system operates as follows. The aircraft transmits a pulsed signal which is received by a constellation of satellites. The pulse time of arrival (TOA) at each satellite depends upon the distance between the aircraft and the satellite. Upon receipt of the pulses, the satellites re-transmit the pulse to a ground station. The ground station then utilizes differences in the TOA's and the known positions of the satellites to calculate the position of the aircraft.

The accuracy of such a system is limited by the accuracy with which the satellite positions are known, by propagation disturbances in the atmosphere and by noise disturbances in the satellite receiver. More specifically the atmospheric and receiver disturbances are translated into TOA errors. The ground station then translates the TOA errors and the satellite position errors into corresponding aircraft position errors.

Considerable previous work [1-5] has been done on calculating the accuracy of such systems. Thus, given disturbance statistics and a specific deployment of a transmitter and receivers, it is straightforward to calculate the resulting rms positional error.

The present report complements previous accuracy work by establishing some useful general principles. Specifically the report asks and answers questions such as the following.

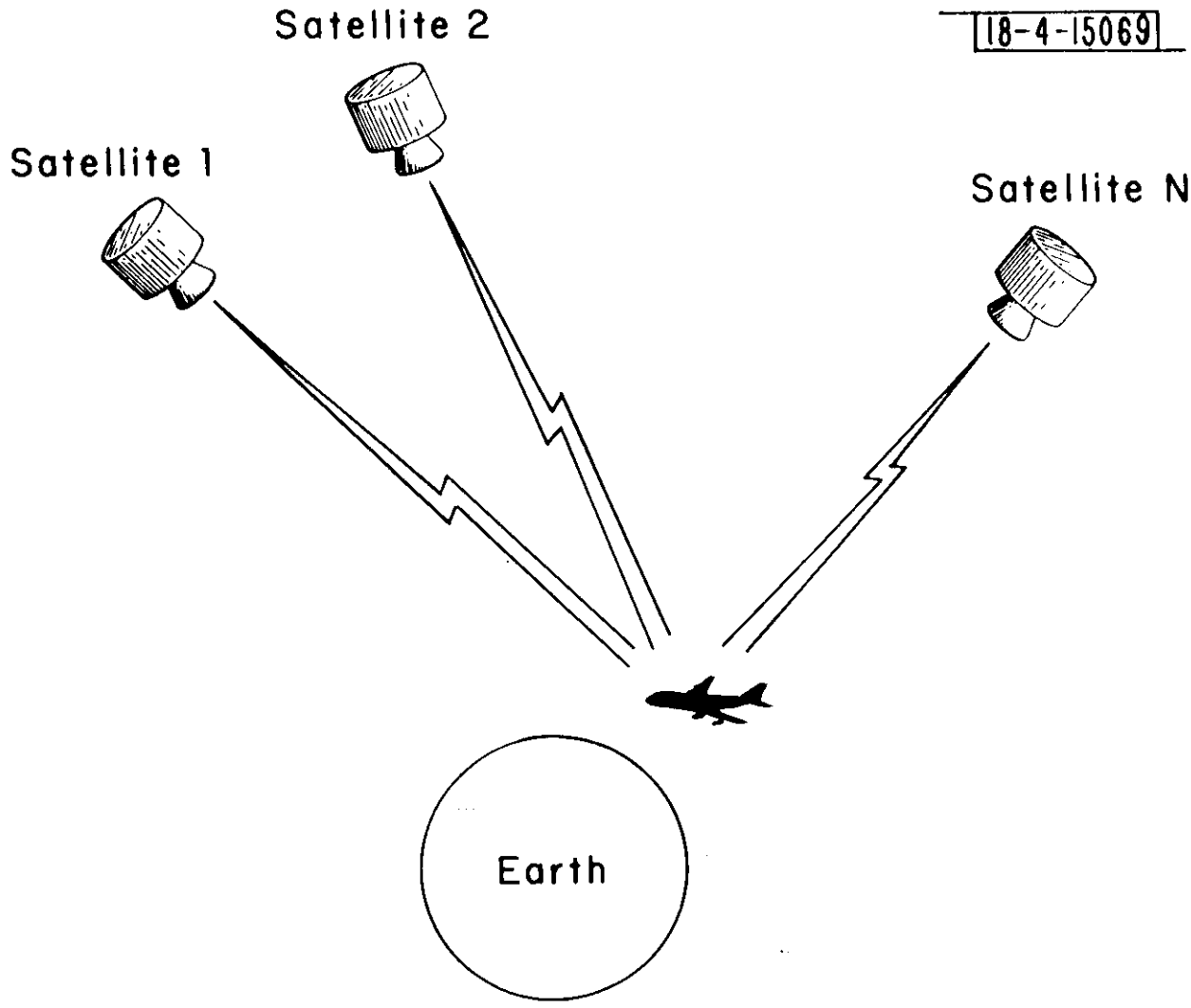

SATELLITE BASED HYPERBOLIC
SURVEILLANCE SYSTEM

Figure 1.1

1. What are the tradeoff's between accuracy and the number of receivers (satellites)?

2. What are the tradeoffs between accuracy and the deployment of the receivers?

3. How do the errors depend on direction? (e.g. in an aircraft surveillance system it is desirable that altitude errors be smaller than horizontal errors. Is this the case?)

4. What are the smallest rms errors that can be attained using a fixed number of receivers? How should the receivers be deployed to achieve minimum error?

5. How is accuracy impaired by dropout of a single receiver? Dropout of which receiver most impairs accuracy?

II. SUMMARY OF RESULTS

Although the present work has been motivated by satellite based surveillance systems like that shown in Figure 1.1, the work is reported in more general terms to make the results available to other applications as well. Thus, it is assumed that a hyperbolic multilateration system consists of a number N of beacons (e.g., satellite receivers), and a subject (e.g., an aircraft). The subject transmits a pulse that is received at different times by the beacons. (Or equivalently, the beacons simultaneously transmit a pulse that is received at different times by the subject). Due to disturbances of various kinds, the TOA's are somewhat in error. Differences in the TOA's then are used to estimate the subject position by means of the conventional least squares principle [5].

It should be noted that the assumption of fixed beacon position ignores the effects of motion in satellite based systems. Thus with regard to such systems, the results reported apply to a single instant of time.

Both two dimensional and three dimensional hyperbolic systems are treated. Two dimensional systems are included not only because of their inherent interest, but also because they provide valuable insight into three dimensional systems.

In some cases no geometrical constraints are placed upon the beacon locations. In other cases the beacon constellations are assumed to be confined to a "viewing sector" (two dimensions) or to a "viewing cone" (three dimensions), or to a plane.

The primary results for three dimensional systems are as follows. Results 1-7 assume that the TOA errors are uncorrelated and have equal variance. Bracketed section and/or example numbers indicate where the results can be found.

1. It is shown that the inverse of the error covariance matrix corresponds to the moment of inertia matrix for a simple mass configuration. The insight provided by this fact makes it

possible to answer many questions relating to accuracy [Section IV].

2. For reasonably uniform cone restricted beacon constellations, it is shown that typical error measures are not highly sensitive to the number N of beacons. Specifically typical error measures are proportional to $1/\sqrt{N}$. Thus, for example, to double system accuracy by the expedient of adding beacons, it is necessary to increase the number of beacons by a factor of four [Section VII].
3. It is shown that accuracy is highly sensitive to cone angle. Thus for example, increasing the half angle of the viewing cone from 40° to 60° can double system accuracy, an improvement that otherwise would require a fourfold increase in the number of beacons [Section VIII].
4. For cone restricted beacon constellations it is shown that altitude errors exceed horizontal position errors, typically by a factor of three [Section IX].
5. Expressions are derived for the minimum attainable RMS errors given N beacons confined to a cone. The expressions are useful for evaluating candidate beacon constellations [Sections X, XI].
6. For cone restricted beacon constellations, system accuracy is most sensitive to dropout of a single beacon either directly overhead or on the cone horizon. If most beacons are directly overhead, then accuracy is most impaired by dropout of a beacon on the horizon. If most beacons are near the horizon, then accuracy is most impaired by dropout of a beacon directly overhead [Section XII].

7. In ground based hyperbolic systems altitude errors substantially exceed ranging errors. Moreover the altitude discrimination provided by such systems is due almost entirely to the beacon nearest the subject [Section VII].
8. The conventional estimate of subject position which assumes uncorrelated equal variance TOA errors is generalized to the case of correlated TOA errors with unequal variances. One practical result is a method for incorporating differences in the received signal to noise ratios into the position estimate [Section XIV].
9. The moment of inertia method for calculating the covariance matrix for positional errors is valid whenever the TOA errors are uncorrelated. Thus many of the results obtained herein for uncorrelated TOA errors having equal variances apply with minor modification to the case of unequal variances [Section XIV].
10. The moment of inertia method for calculating the inverse of the error covariance matrix is generalized to accommodate an independent (e.g., barometric) altitude measurement [Section XV].

Analogous results are obtained for two dimensional problems.

The report is written utilizing an example format. Some examples draw major conclusions. Other examples serve to amplify earlier results, or provide a basis for subsequent ones.

III. EQUATIONS FOR ACCURACY MEASURES

The basic accuracy measures for a hyperbolic multilateration system are derived in this section. The derivation follows that given in References [2,4,5]. The derivation is carried out for the three dimensional case. All equations apply with obvious modifications to the two dimensional case as well.

A typical hyperbolic system is shown in Figure 3.1. The equations relating the pulse times of arrival to the distances $d_1, d_2, \ldots d_N$ are as follows.

$$\begin{aligned} \tau_1 - \varepsilon_1 &= \tau_o + d_1/c \\ &\vdots \\ \tau_N - \varepsilon_N &= \tau_o + d_N/c \end{aligned} \tag{3.1}$$

where

τ_j = The recorded time of arrival (TOA) of the pulse at the jth beacon

ε_j = the error term which accounts for disturbances in the medium through which the pulse propagates, and noise disturbances in the receiver

$\tau_j - \varepsilon_j$ = the time at which the pulse would arrive at beacon j where no disturbances present

τ_o = the time at which the pulse is transmitted

d_j/c = the ideal pulse transit time from the subject to beacon j (c denotes the pulse velocity)

It is assumed that the τ_j are corrected for all known biases so that the ε_j have zero mean.

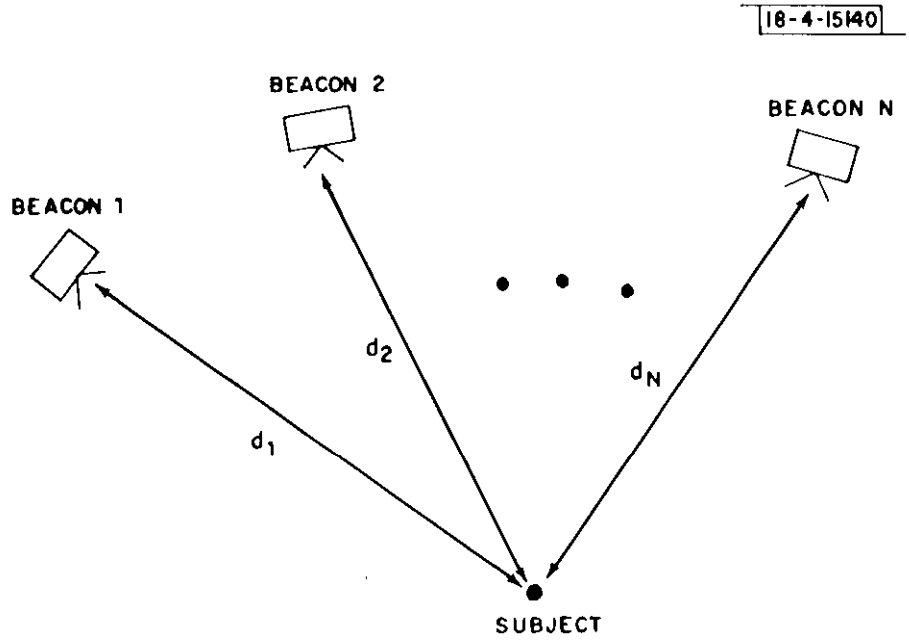

Figure 3.1

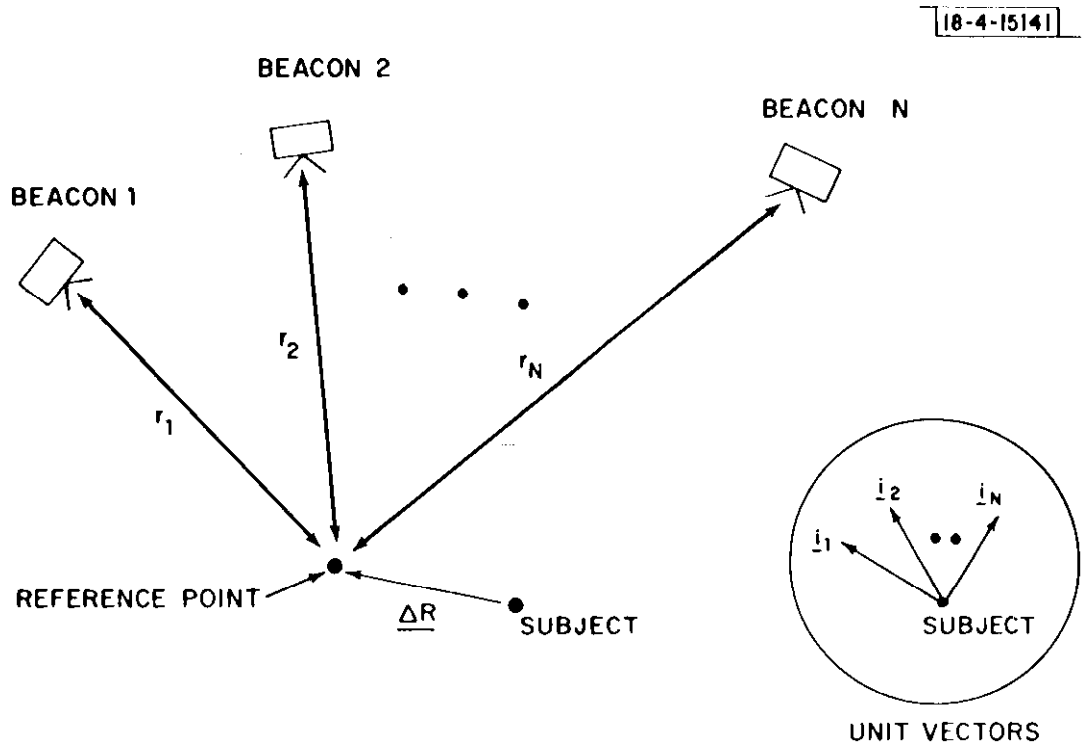

Figure 3.2

Equations (3.1) are non-linear when expressed in terms of any convenient coordinate system. For example, use of a cartesian coordinate system replaces the distance d_j by a quantity of the form $\sqrt{(X_j - X_o)^2 + (Y_j - Y_o)^2 + (Z_j - Z_o)^2}$. Thus Equations (3.1) are difficult to solve for the subject coordinates. The approach selected here for placing (3.1) into a tractable form* consists of linearizing (3.1) about a convenient reference point as shown in Figure 3.2. The equations then take the form

$$\begin{aligned} \tau_1 - \varepsilon_1 &= \tau_o + r_1/c + \underline{i}_1 \cdot \underline{\Delta R}/c \\ &\vdots \\ \tau_N - \varepsilon_N &= \tau_o + r_N/c + \underline{i}_N \cdot \underline{\Delta R}/c \end{aligned} \tag{3.2}$$

where

$\underline{\Delta R}$ = a vector** specifying subject position with respect to the reference point

$\underline{i}_j$ = a unit vector pointing from the subject to beacon j

It is assumed that the vector $\underline{\Delta R}$ is expressed in terms of some convenient cartesian coordinate system (X', Y', Z').

Except for the corrections ε_j, Equations (3.2) comprise a system of N linear equations in N unknowns, the unknowns being τ_o and the three components of $\underline{\Delta R}$. The equations can be simplified by subtracting each equation from its predecessor; this serves to eliminate the (unknown) quantity τ_o. The resultant equations take the form

$$\begin{aligned} (\tau_1 - \tau_2) + (\varepsilon_1 - \varepsilon_2) &= (r_1 - r_2)/c + (\underline{i}_1 - \underline{i}_2) \cdot \underline{\Delta R}/c \\ &\vdots \\ (\tau_{N-1} - \tau_N) + (\varepsilon_{N-1} - \varepsilon_N) &= (r_{N-1} - r_N)/c + (\underline{i}_{N-1} - \underline{i}_N) \cdot \underline{\Delta R}/c \end{aligned} \tag{3.3}$$

---

*This step follows that in References [2,4,5].

**An underbar "——" is employed throughout to designate vector or matrix quantities.

Because the correction terms ε_j are unknown, it is impossible to solve (3.3) exactly for the subject position $\underline{\Delta R}$. The best that can be done is to derive from (3.3) a meaningful estimate $\underline{\Delta R}^*$ of the subject position $\underline{\Delta R}$.

The system (3.3) comprises N-1 linear equations in three unknowns. One method of estimating $\underline{\Delta R}$ is to

i) select three of the equations and ignore the remainder
ii) set the correction terms ε_j equal to zero (i.e., their mean values) in the selected equations
iii) solve the resulting set of three equations in three unknowns for the estimate $\underline{\Delta R}^*$ of $\underline{\Delta R}$.

While this approach is conceptually simple, it discards valuable information, and eliminates the possibility of error cancellation.

A more profitable approach consists of

i) averaging the N-1 equations together to obtain three equations
ii) setting the ε_j equal to zero in the averaged equations
iii) solving the resultant system of three equations in three unknowns for an estimate $\underline{\Delta R}^*$ of $\underline{\Delta R}$.

For purposes of averaging Equations (3.3) together, it is convenient to re-write (3.3) using matrix notation. The matrix counterpart of (3.3) is

$$\underline{\Delta T} - \underline{H}\,\underline{\varepsilon} = \frac{1}{c}\,\underline{H}\,\underline{R} + \frac{1}{c}\,\underline{H}\,\underline{F}\,\underline{\Delta R} \qquad (3.4)$$

where

$\underline{\Delta T}$ = an N-1 element vector the jth element of which equals the TOA difference $\tau_j - \tau_{j+1}$

$\underline{\varepsilon}$ = an N element vector the jth element of which equals ε_j

$\underline{R}$ = an N element vector the jth element of which equals r_j

$\underline{F}$ = an N x 3 matrix the jth row of which contains the three components of the unit vector $\underline{i}_j$ pointing to the jth beacon

$\underline{H}$ = an N-1 x N matrix of the form

$$\left[\begin{array}{ccccccc} 1 & -1 & 0 & \cdots & & 0 \\ 0 & 1 & -1 & & & 0 \\ \cdot & \cdot & \cdot & & & \cdot \\ \cdot & \cdot & \cdot & & & \cdot \\ 0 & 0 & 0 & 0 & 1 & -1 \end{array}\right] \Bigg\} \text{N-1 rows}$$

N columns

The averaging procedure selected here consists of pre-multiplying (3.4) by the 3 x N matrix $\underline{F}'\ \underline{H}'\ (\underline{H}\ \underline{H}')^{-1}$ where the prime denots matrix transposition. The resulting equation for the estimate $\underline{\Delta R}^*$ is given by

$$\underline{F}'\ \underline{H}'(\underline{H}\ \underline{H}')^{-1}\ \underline{\Delta T} - \underline{F}'\ \underline{H}'(\underline{H}\ \underline{H}')^{-1}\ \underline{H}\ \underline{R} = \underline{F}'\ \underline{H}'(\underline{H}\ \underline{H}')^{-1}\ \underline{H}\ \underline{F}\ \underline{\Delta R}^* \quad (3.5)$$

This averaging decision follows References [2,4,5,8] and amounts to selecting the position estimate $\underline{\Delta R}^*$ as that position which requires the smallest total squared error $\underline{\varepsilon}'\ \underline{\varepsilon}$ to account for the observed data (i.e., the τ_j and r_j).

In the case where the ε_j can be represented as uncorrelated Gaussian random variables with equal variances, the averaging decision is equivalent to use of a maximum likelihood estimate since the multivariate probability density function $\rho_{\underline{\varepsilon}}$ then takes the form

$$\rho_{\underline{\varepsilon}} = \frac{1}{(2\pi\sigma_\tau^2)^{N/2}} \exp\left(-\underline{\varepsilon}'\,\underline{\varepsilon}/2\sigma_\tau^2\right) \tag{3.6}$$

The resulting position estimate $\underline{\Delta R}^*$ is given by

$$\begin{aligned}\underline{\Delta R}^* = {} & c\,[\underline{F}'\,\underline{H}'(\underline{H}\,\underline{H}')^{-1}\,\underline{H}\,\underline{F}]^{-1}\,\underline{F}'\,\underline{H}'(\underline{H}\,\underline{H}')^{-1}\,\underline{\Delta T} \\ & - [\underline{F}'\,\underline{H}'(\underline{H}\,\underline{H}')^{-1}\,\underline{H}\,\underline{F}]^{-1}\,\underline{F}'\,\underline{H}'(\underline{H}\,\underline{H}')^{-1}\,\underline{H}\,\underline{R}\end{aligned} \tag{3.7}$$

A relatively straightforward calculation shows that the position errors that result from use of the estimate (3.7) are

$$(\underline{\Delta R}^* - \underline{\Delta R}) = c\,[\underline{F}'\,\underline{H}'\,(\underline{H}\,\underline{H}')^{-1}\,\underline{H}\,\underline{F}]^{-1}\,\underline{F}'\,\underline{H}'(\underline{H}\,\underline{H}')^{-1}\,\underline{H}\,\underline{\varepsilon} \tag{3.8}$$

Consequently the covariance matrix $\underline{P}_{\Delta R}$ for the position error is given by

$$\begin{aligned}\underline{P}_{\Delta R} &= \overline{(\underline{\Delta R}^* - \underline{\Delta R})(\underline{\Delta R}^* - \underline{\Delta R})'} \\ &= (\sigma_\tau c)^2\,[\underline{F}'\,\underline{H}'(\underline{H}\,\underline{H}')^{-1}\,\underline{H}\,\underline{F}]^{-1}\end{aligned} \tag{3.9}$$

The quantity σ_τ in (3.9) denotes the rms error in the TOA recorded at a typical beacon [i.e., $\sigma_\tau^2 = \overline{(\varepsilon_j)^2}$ for $j = 1,2,\ldots N$]. Thus the factor $(\sigma_\tau c)^2$ denotes the mean squared ranging error implied by the TOA error.

It is convenient to express the covariance matrix (3.9) as follows

$$\underline{P}_{\Delta R} = (\sigma_\tau c)^2\,\underline{\Gamma} \tag{3.10}$$

$$= (\sigma_\tau c)^2 \begin{bmatrix} \Gamma_{xx} & \Gamma_{xy} & \Gamma_{xz} \\ \Gamma_{xy} & \Gamma_{yy} & \Gamma_{yz} \\ \Gamma_{xz} & \Gamma_{yz} & \Gamma_{zz} \end{bmatrix} \tag{3.11}$$

This formulation is useful because it places in evidence the elements of the matrix

$$[\underline{F}' \, \underline{H}' \, (\underline{H} \, \underline{H}')^{-1} \, \underline{H} \, \underline{F}]^{-1} \triangleq \underline{\Gamma} \tag{3.12}$$

All of the conventional measures of accuracy are directly available from (3.11). For example, the mean squared errors in the X, Y and Z directions are given respectively by

$$\sigma_x^2 = (\sigma_\tau c)^2 \, \Gamma_{xx} \tag{3.13}$$

$$\sigma_y^2 = (\sigma_\tau c)^2 \, \Gamma_{yy} \tag{3.14}$$

$$\sigma_z^2 = (\sigma_\tau c)^2 \, \Gamma_{zz} \tag{3.15}$$

Similarly the total mean squared error σ^2, and the so-called "geometric dilution of precision" (GDOP) are given by

$$\sigma^2 = \sigma_x^2 + \sigma_y^2 + \sigma_z^2 = (\sigma_\tau c)^2 (\Gamma_{xx} + \Gamma_{yy} + \Gamma_{zz}) \tag{3.16}$$

and

$$\text{GDOP} = \frac{\sigma}{\sigma_\tau c} = (\Gamma_{xx} + \Gamma_{yy} + \Gamma_{zz})^{1/2} \tag{3.17}$$

Equations (3.13-3.17) show that the elements of the Γ matrix in (3.10) posses a simple interpretation. Specifically the elements can be interpreted as error magnification factors. For example, Equation (3.13) asserts that the mean squared error in the X direction equals the mean squared ranging

error magnified by the factor ($\Gamma_{xx} + \Gamma_{yy} + \Gamma_{zz}$). Accordingly the matrix $\underline{\Gamma}$ henceforth is called the error magnification matrix.

IV. THE INVERSE ERROR MAGNIFICATION MATRIX

To deduce useful properties of the various measures of positional error, it is necessary to relate the error magnification matrix $\underline{\Gamma}$ or some function of it to the beacon-subject geometry. The present section shows that the inverse of $\underline{\Gamma}$ possesses two extremely simple interpretations in terms of system geometry. It is these interpretations that lead to the conclusions summarized in Section II.

Thus let $\underline{L}$ denote $\underline{\Gamma}^{-1}$. That is, let

$$\begin{aligned} \underline{L} &= \underline{F}' \underline{H}' (\underline{H} \underline{H}')^{-1} \underline{H} \underline{F} \\ &= \underline{F}' \underline{H}' (\underline{H} \underline{H}')^{-1} \underline{H} \underline{H}' (\underline{H} \underline{H}')^{-1} \underline{H} \underline{F} \\ &= [\underline{H}' (\underline{H} \underline{H}')^{-1} \underline{H} \underline{F}]^{1} [\underline{H}' (\underline{H} \underline{H}')^{-1} \underline{H} \underline{F}] \\ &= \underline{K}' \underline{K} \end{aligned} \tag{4.1}$$

where

$$\underline{K} = \underline{H}' (\underline{H} \underline{H}')^{-1} \underline{H} \underline{F} \tag{4.2}$$

Straightforward multiplication shows that

$$\underline{H}' (\underline{H} \underline{H}')^{-1} \underline{H} = \underline{I} - \frac{1}{N} \begin{bmatrix} 1 & 1 & .. & 1 \\ 1 & 1 & .. & 1 \\ \vdots & \vdots & & \vdots \\ 1 & 1 & .. & 1 \end{bmatrix} \tag{4.3}$$

where $\underline{I}$ denotes the identity matrix. Thus

$$\underline{K} = \left(\underline{I} - \frac{1}{N} \begin{bmatrix} 1 & 1 & .. & 1 \\ 1 & 1 & .. & 1 \\ \vdots & \vdots & & \vdots \\ 1 & 1 & .. & 1 \end{bmatrix} \right) \underline{F} = \begin{bmatrix} \underline{i}_1' - \overline{\underline{i}}' \\ \underline{i}_2' - \overline{\underline{i}}' \\ \vdots \\ \underline{i}_N' - \overline{\underline{i}}' \end{bmatrix} \tag{4.4}$$

when $\underline{i}_j'$ denotes the jth unit vector in row format, and

$$\underline{\bar{i}} = \frac{1}{N} \sum_{j=1}^{N} \underline{i}_j \tag{4.5}$$

To interpret the matrix $\underline{L}$, assume that the following construction is carried out.

Construction of Beacon Images on Unit Sphere

i) draw a sphere of unit radius with center at an origin 0

ii) draw the vectors $\underline{i}_1, \underline{i}_2 \ldots \underline{i}_N$ from the origin 0

iii) place unit masses at the points $p_1, p_2, \ldots p_N$ where the unit vectors terminate in the sphere (see Figure 4.1)

The vector $\underline{\bar{i}}$ specified by (4.5) can be interpreted as pointing from the origin 0 to the center of mass CM of the mass configuration as shown in Figure 4.1. Likewise the vector difference $\underline{i}_j' - \underline{\bar{i}}'$ contained in the jth row of the matrix $\underline{K}$ can be interpreted as a vector pointing from CM to the unit mass at point p_j. Thus if X,Y,Z denotes a cartesian coordinate system centered at CM, and differing from the system (X', Y', Z') only by a translation, then the elements of the jth row of $\underline{K}$ are simply the coordinates X_j, Y_j and Z_j of the point P_j in the system (X,Y,Z).

That is,

$$\underline{K} = \begin{bmatrix} 1 & 1 & 1 \\ 2 & 2 & 2 \\ \vdots & \vdots & \vdots \\ X_N & Y_N & Z_N \end{bmatrix} \tag{4.6}$$

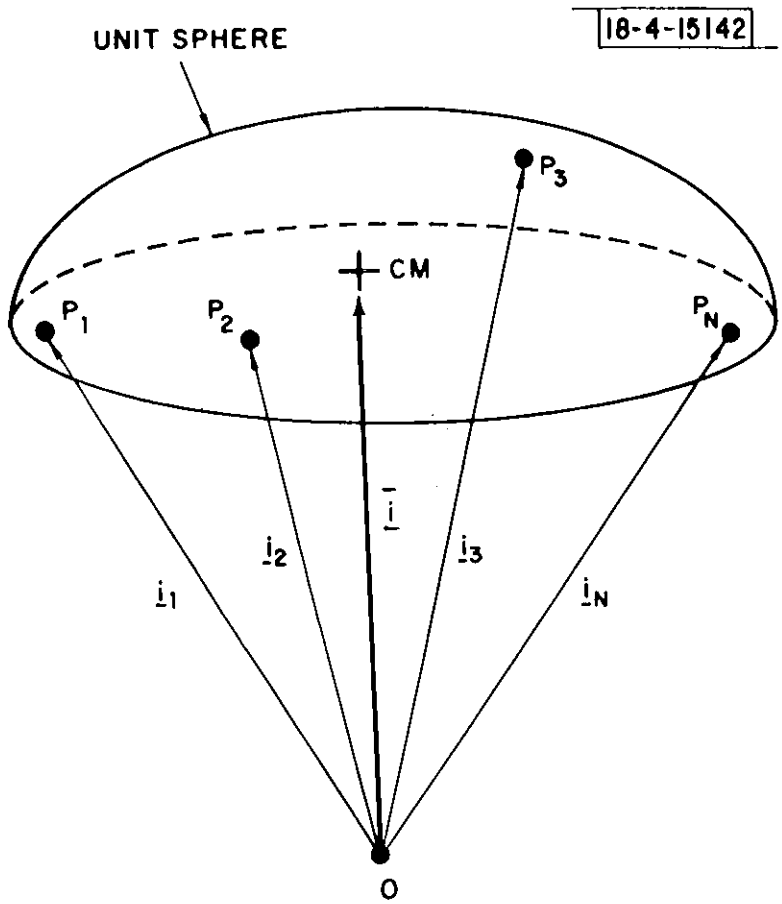

Figure 4.1

The desired formulation of $\underline{L}$ follows directly from (4.1) and (4.6), namely

$$\underline{L} = \begin{bmatrix} \sum_{j=1}^{N} X_j^2 & \sum_{j=1}^{N} Y_j X_j & \sum_{j=1}^{N} Z_j Y_j \\ \sum_{j=1}^{N} X_j Y_j & \sum_{j=1}^{N} Y_j^2 & \sum_{j=1}^{N} Z_j Y_j \\ \sum_{j=1}^{N} X_j Z_j & \sum_{j=1}^{N} Y_j Z_j & \sum_{j=1}^{N} Z_j^2 \end{bmatrix} \tag{4.7}$$

In some cases it is useful to re-write (4.7) as follows.

$$L = N \begin{bmatrix} \frac{1}{N} \sum_{j=1}^{N} X_j^2 & \frac{1}{N} \sum^{N} Y_j^2{}_j & \frac{1}{N} \sum^{N} Z_j X_j \\ \frac{1}{N} \sum_{j=1}^{N} X_j Y_j & \frac{1}{N} \sum_{j=1}^{N} Y_j^2 & \frac{1}{N} \sum_{j=1}^{N} Z_j Y_j \\ \frac{1}{N} \sum_{j=1}^{N} X_j Z_j & \frac{1}{N} \sum_{j=1}^{N} Y_j Z_j & \frac{1}{N} \sum_{j=1}^{N} Z_j^2 \end{bmatrix} \tag{4.8}$$

Equation (4.7) asserts that the entries in $\underline{L}$ are simply the moments and products of inertia of the unit mass configuration about its center of mass.

By contrast Equation (4.8) asserts that the entries in $\underline{L}$ can be regarded as averages of the second order products X^2, Y, Z etc. over the set of points P_1, P_2,...P_N.

Both interpretations are highly valuable as they make it possible to apply insights gained from the fields of mechanics and statistics to the accuracy problem.

The two dimensional counterparts of (4.7) and (4.8) are as follows.

$$\underline{L} = \begin{bmatrix} \sum_{j=1}^{N} X_j^2 & \sum_{j=1}^{N} X_j Y_j \\ \sum_{j=1}^{N} X_j Y_j & \sum_{j=1}^{N} Y_j^2 \end{bmatrix} \tag{4.9}$$

$$= N \begin{bmatrix} \frac{1}{N} \sum_{j=1}^{N} X_j^2 & \frac{1}{N} \sum_{j=1}^{N} X_j Y_j \\ \frac{1}{N} \sum_{j=1}^{N} X_j Y_j & \frac{1}{N} \sum_{j=1}^{N} Y_j^2 \end{bmatrix} \tag{4.10}$$

In formulating (4.9) and (4.10) the sphere of unit radius is replaced by a circle of unit radius. Otherwise points P_1, P_2,...P_N and CM are constructed as before. Again the quantities X_j, Y_j denote the coordinates of point P_j measured from CM.

The interpretations of Equations (4.7) and (4.8) apply without change to (4.9) and (4.10).

V. CALCULATION OF THE ERROR MAGNIFICATION MATRIX

Five examples are given in this section to illustrate the ease with which the error magnification matrix $\underline{\Gamma}$ and typical error measures can be calculated.

A review of Sections III and IV will show that the orientation of the coordinate system (X,Y,Z) can be chosen freely. Accordingly the coordinate systems here are selected to produce a diagonal $\underline{\Gamma}$. This choice further simplifies the calculations.

Example 5.1 Consider a two dimensional constellation of four beacons having equal ninety degree azimuth separations from the subject.

The unit vectors $\underline{i}_1..\underline{i}_4$ and the points $P_1..P_4$ for the constellation are shown in Fig. 5.1.

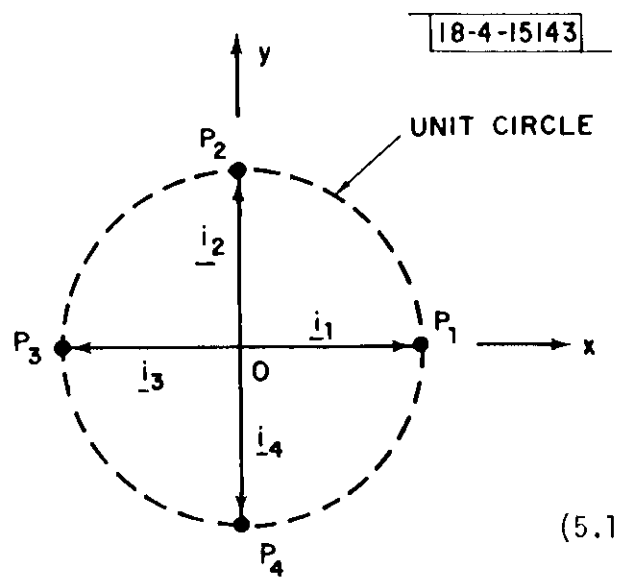

Figure 5.1

Clearly the center of mass CM of points $P_1..P_4$ is at the origin. Thus

$$\sum X_j^2 = \sum Y_j^2 = 2 \tag{5.1}$$

$$\sum X_j Y_j = 0 \tag{5.2}$$

Accordingly the inverse of $\underline{\Gamma}$ is given by

$$\underline{L} = \begin{bmatrix} 2 & 0 \\ 0 & 2 \end{bmatrix} \tag{5.3}$$

Inversion of (5.3) gives

$$\underline{\Gamma} = \underline{L}^{-1} = \begin{bmatrix} 1/2 & 0 \\ 0 & 1/2 \end{bmatrix} \tag{5.4}$$

All error measures of interest are immediately available from (5.4) as indicated in Section III. For example

$$\sigma_x^2 = \sigma_y^2 = \frac{1}{2}(c\sigma_\tau)^2 \tag{5.5}$$

$$\sigma^2 = (c\sigma_\tau)^2 (1/2 + 1/2) = (c\sigma_\tau)^2 \tag{5.6}$$

$$\text{GDOP} = 1 \tag{5.7}$$

END OF EXAMPLE

Example 5.2 Consider a two dimensional constellation of three beacons having equal one hundred twenty degree separations from the subject. The unit vectors $\underline{i}_1 .. \underline{i}_3$ and the points $P_1 .. P_3$ for the constellation are shown in Figure 5.2.

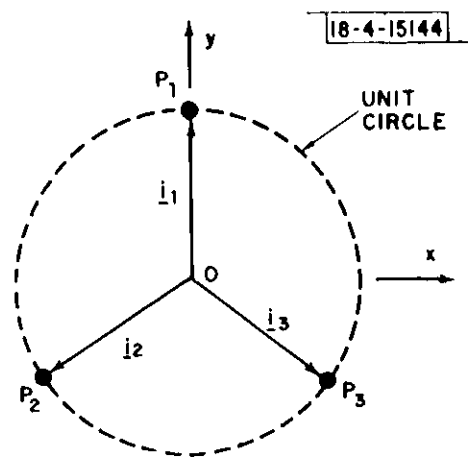

Figure 5.2

Once again the CM is at the origin. Therefore

$$\sum X_j^2 = \sum Y_j^2 = \frac{3}{2} \tag{5.8}$$

$$\sum X_j Y_j = 0 \tag{5.9}$$

Consequently

$$\underline{L} = \begin{bmatrix} 3/2 & 0 \\ 0 & 3/2 \end{bmatrix} \quad \text{and} \quad \underline{\Gamma} = \underline{L}^{-1} = \begin{bmatrix} 2/3 & 0 \\ 0 & 2/3 \end{bmatrix} \tag{5.10a, 5.10b}$$

Thus, for example

$$\sigma_x^2 = \frac{2}{3}(c\sigma_\tau)^2 \tag{5.11}$$

$$\text{GDOP} = \left(\frac{2}{3} + \frac{2}{3}\right)^{1/2} = 2/\sqrt{3} \tag{5.12}$$

END OF EXAMPLE

Example 5.3 Consider a (degenerate) two dimensional constellation consisting of three beacons in a straight line with the subject. Assume the subject is located between the extreme beacons.

The vectors $\underline{i}_1 .. \underline{i}_3$ and the points $\underline{P}_1 .. \underline{P}_3$ for the constellation are shown in Fig. 5.3.

In this case the center of mass CM is not at the origin O. Instead CM is a distance 1/3 to the right of O as shown.

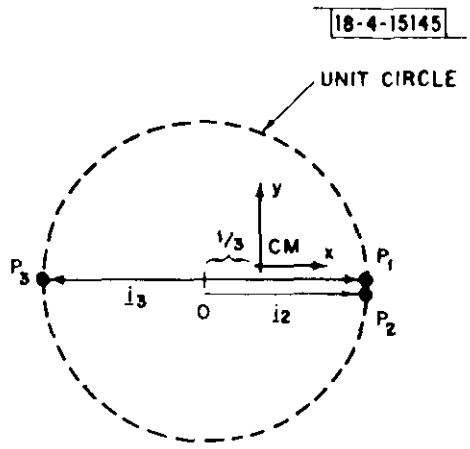

Figure 5.3

The second moments about CM are as follows

$$\sum X_j^2 = 2\left(\frac{2}{3}\right)^2 + \left(\frac{4}{3}\right)^2 = 24/9 \tag{5.13}$$

$$\sum Y_j^2 = 0 \tag{5.14}$$

$$\sum X_j Y_j = 0 \tag{5.15}$$

Consequently

$$\underline{L} = \begin{bmatrix} 24/9 & 0 \\ 0 & 0 \end{bmatrix} \quad \text{and} \quad \underline{\Gamma} = \underline{L}^{-1} = \begin{bmatrix} 9/24 & \infty \\ \infty & \infty \end{bmatrix} \tag{5.16a, 5.16b}$$

so that

$$\sigma_x^2 = \frac{9}{24} (c\sigma_\tau)^2 \tag{5.17}$$

$$\sigma_y^2 = \infty \tag{5.18}$$

$$\text{GDOP} = \infty \tag{5.19}$$

Note: It is easy to see that the $\underline{\Gamma}$ matrix contains infinite elements whenever the beacon images $P_1..P_N$ lie in a straight line (two dimensions) or in a plane (three dimensions). The reasoning is as follows. In such cases the center of mass CM of the points $P_1..P_N$ is located on the same line as $P_1..P_N$ (two dimensions) or in the same plane as $P_1..P_N$ (three dimensions). Thus the coordinate system at CM can be selected so that one axis, say the Y axis, is normal to the line or plane defined by $P_1..P_N$. The entries in the Y row and Y column of $\underline{L}$ then are zero so that $\underline{L}$ is singular and $\underline{\Gamma}$ contains infinite elements. Since the $\underline{\Gamma}$ matrix for any other cartesian coordinate system centered at CM is identical to that just discussed except for an orthogonal transformation, the $\underline{\Gamma}$ matrices for all such systems contain infinite elements.

END OF EXAMPLE

Example 5.4 (See Appendix I, Reference [5]) Consider a three dimensional constellation consisting of four beacons positioned within a cone as shown in Figure 5.4.

18-4-15146

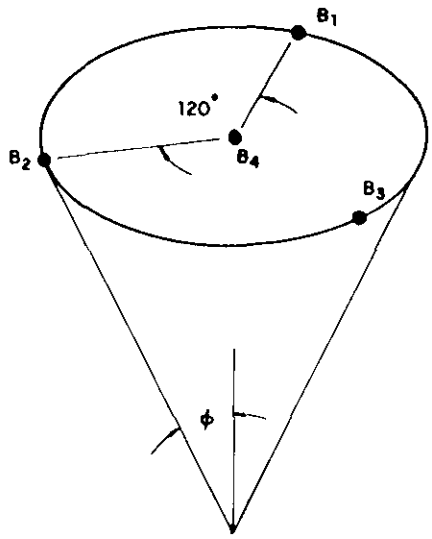

Figure 5.4

Figure 5.5 depicts the unit vectors $\underline{i}_1 \cdots \underline{i}_4$ and the points $P_1 \cdots P_4$.

A straightforward calculation shows that the center of mass CM is a distance 3/4 (1-cos ϕ) from point P_4 as shown.

The $\underline{L}$ matrix is made diagonal by selecting a coordinate system (X,Y,Z) at CM such that the z axis coincides with $\underline{i}_4$, and the Y axis is co-planar with $\underline{i}_1$ and $\underline{i}_4$.

The element L_{zz} of $\underline{L}$ is given by

$$L_{zz} = [3(\tfrac{1}{4})^2 + (\tfrac{3}{4})^2](1-\cos\phi)^2$$

$$= \frac{3}{4}(1-\cos\phi)^2 \qquad (5.20)$$

18-4-15147

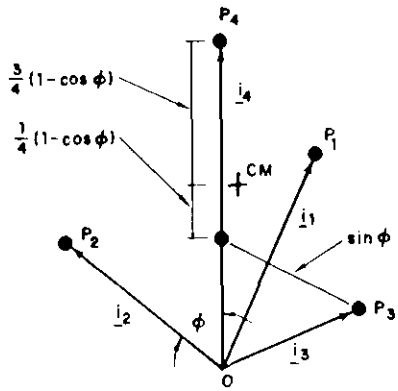

Figure 5.5

The results of Example 5.2 can be used to calculate the remaining diagonal ements L_{xx} and L_{yy} if it is noted that the projection of the vectors $\underline{i}_1$, $\underline{i}_2$ and $\underline{i}_3$ onto a plane normal to $\underline{i}_4$ is identical to Figure 5.2 except for a scale factor of sin ϕ. Specifically

$$L_{xx} = L_{yy} = \frac{3}{2}\sin^2\phi \qquad (5.21)$$

Consequently

$$L = \begin{bmatrix} \frac{3}{2}\sin^2\phi & 0 & 0 \\ 0 & \frac{3}{2}\sin^2\phi & 0 \\ 0 & 0 & \frac{3}{4}(1-\cos\phi)^2 \end{bmatrix} \tag{5.22}$$

Thus the error magnification matrix is given by

$$\underline{\Gamma} = \begin{bmatrix} \frac{2}{3}\frac{1}{\sin^2\phi} & 0 & 0 \\ 0 & \frac{2}{3}\frac{1}{\sin^2\phi} & 0 \\ 0 & 0 & \frac{4}{3}\frac{1}{(1-\cos\phi)^2} \end{bmatrix} \tag{5.23}$$

All error measures are immediately available from (5.23). For example

$$\begin{aligned} \text{GDOP} &= \left[(2)\frac{2}{3}\frac{1}{\sin^2\phi} + \frac{4}{3}\frac{1}{(1-\cos\phi)^2}\right]^{1/2} \\ &= \sqrt{\frac{8}{3(1-\cos\phi)^2(1+\cos\phi)}} \end{aligned} \tag{5.24}$$

END OF EXAMPLE

Example 5.5 Consider a fifteen beacon constellation having images $P_1, \ldots P_{15}$ on the unit sphere as shown in Figure 5.6

The X' and Y' coordinates of CM are zero due to symmetry. The Z' coordinate of CM can be determined by examining the Z' axis distribution of mass as shown in Figure 5.7. A straightforward calculation shows that CM is located a distance

$$Z' = .35 \tag{5.25}$$

from the origin O.

Selection of the (X, Y, Z) coordinate system to coincide with the (X', Y',Z') system except for an upward translation to CM produces a diagonal $\underline{L}$ matrix.

The entry L_{zz} can be calculated directly from Figure 5.7. Specifically

$$\begin{aligned} L_{zz} &= \sum_{j=1}^{15} (Z_j)^2 \\ &= 1\ (.65)^2 + 6(.357)^2 + 8(.35)^2 \\ &= 2.16 \end{aligned} \tag{5.26}$$

The entries L_{xx} and L_{yy} can be evaluated most easily by taking advantage of symmetry and the pythagorean theorem for the typical point P_j. The pythagorean theorem asserts that

$$(X_j')^2 + (Y_j') + (Z_j')^2 = 1 \tag{5.27}$$

Summation of (5.27) over all fifteen P_j yields

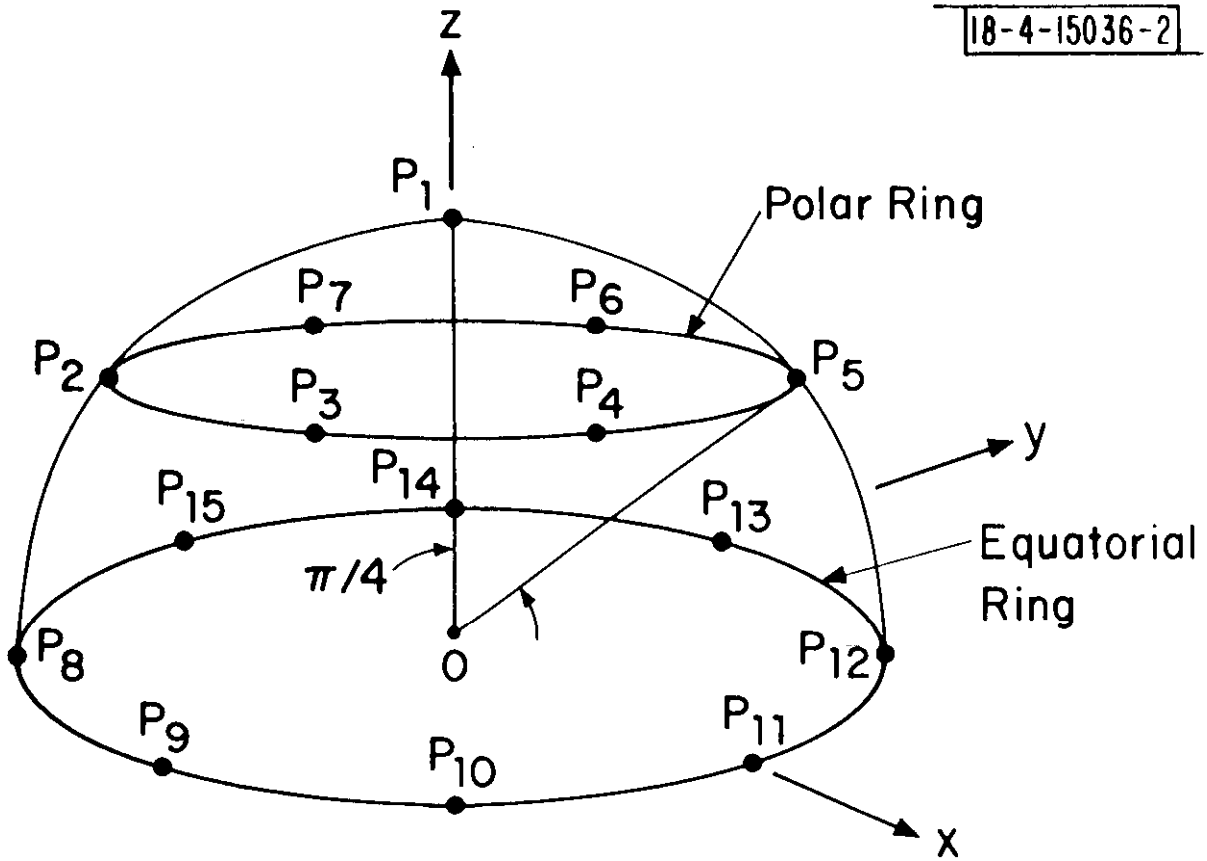

Figure 5.6

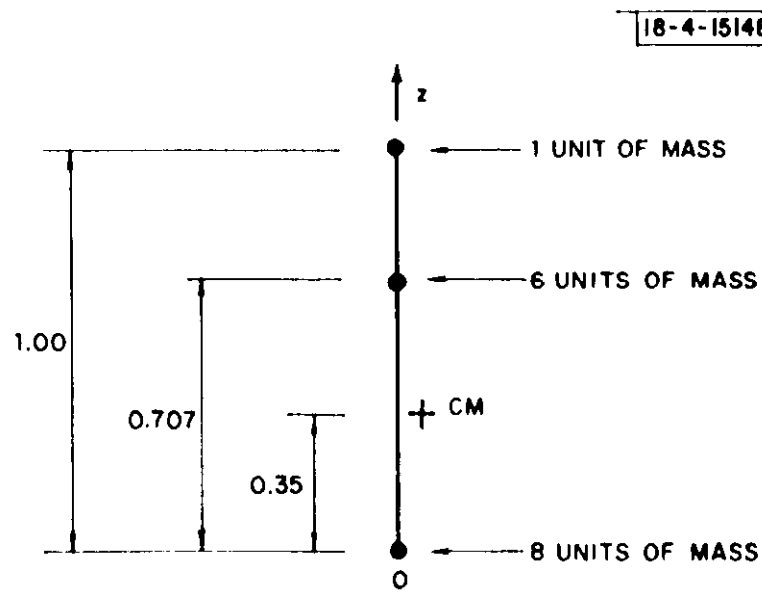

Figure 5.7

$$\sum_{j=1}^{15} (X'_j)^2 + \sum_{j=1}^{15} (Y'_j)^2 + \sum_{j=1}^{15} (Z'_j)^2 = 15 \tag{5.28}$$

Because the (X,Y,Z) and (X',Y',Z') coordinate systems differ only by a translation in the z direction.

$$\sum_{j=1}^{15} (X'_j)^2 = \sum_{j=1}^{15} (X_j)^2 = L_{xx} \tag{5.29}$$

$$\sum_{j=1}^{15} (Y'_j)^2 \quad \sum_{j=1}^{15} (Y_j)^2 = L_{yy} \tag{5.30}$$

Moreover straightforward calculation from Figure 5.7 shows that

$$\sum_{j=1}^{15} (Z'_j)^2 = 6(.707)^2 + 1(1)^2 = 4 \tag{5.31}$$

Use of (5.29), (5.30) and (5.31) in (5.28) shows that

$$L_{xx} + L_{yy} = 11 \tag{5.32}$$

But $L_{xx} = L_{yy}$ by symmetry. As a result

$$L_{xx} = L_{yy} = 5.5 \tag{5.33}$$

Consequently the inverse error magnification matrix is given by

$$\underline{L} = \begin{bmatrix} 5.5 & 0 & 0 \\ 0 & 5.5 & 0 \\ 0 & 0 & 2.16 \end{bmatrix} \tag{5.34}$$

so that

$$\underline{\Gamma} = \begin{bmatrix} .182 & 0 & 0 \\ 0 & .182 & 0 \\ 0 & 0 & .463 \end{bmatrix} \tag{5.35}$$

Thus for example the error measures $\sigma_z^2/(c\sigma_\tau)^2$ and GDOP are given by

$$\sigma_z^2/(c\sigma_\tau)^2 = .463 \tag{5.36}$$

$$\text{GDOP} = (.182 + .182 + .463)^{1/2}$$

$$= .910$$

END OF EXAMPLE

VI. APPROXIMATE CALCULATION OF $\underline{\Gamma}$

Approximate expressions for error measures are very useful for assessing trade-offs between accuracy and other system parameters. This section contains five examples that show how approximate expressions can be derived.

The basic idea behind calculating approximate error measures is to approximate the $\underline{L}$ matrix (4.8) or (4.10), and then extract error measures from $\underline{\Gamma} = \underline{L}^{-1}$ as described in Section III.

The approximation of the $\underline{L}$ matrix simply involves replacing all discrete averages in (4.8) or (4.10) by corresponding continuous integral averages. In two dimensional problems the resulting integrals represent averages of the products X^2, X,Y and Y^2 over a sector of a unit circle centered at the subject. In three dimensional problems the resulting integrals represent similar averages over a portion of a unit sphere centered at the subject. The quantities X,Y,Z continue to be measured from the center of mass (rather the origin 0).

Once again the coordinate systems in the examples are selected to produce a diagonal $\underline{L}$ matrix.

Example 6.1 (Circular Constellation) Consider a two dimensional beacon constellation consisting of N beacons equally spaced in azimuth.

The array of vectors $\underline{i}_1 .. \underline{i}_N$ and points $P_1 .. P_N$ for case N=8 are shown in Figure 6.1. Clearly the CM is at the origin 0.

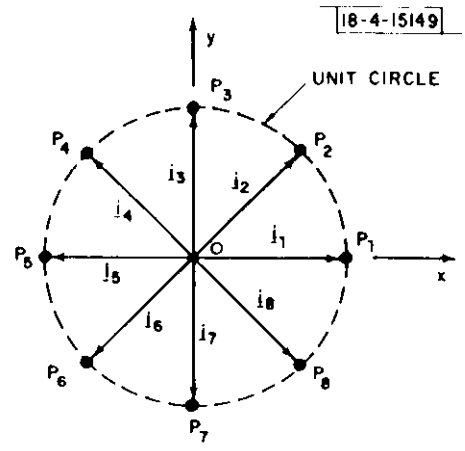

Figure 6.1

The X-X element of the matrix (4.10) can be approximated as follows

$$\frac{1}{N}\sum_{j=1}^{N} X_j^2 \approx \frac{\oint_{\text{unit circle}} X^2\, ds}{\oint_{\text{unit circle}} ds}$$

$$= 1/2 \tag{6.1}$$

Similarly

$$\frac{1}{N}\sum_{j=1}^{N} X_j Y_j \approx \frac{\oint_{\text{unit circle}} XY\, ds}{\oint_{\text{unit circle}} ds} = 0 \tag{6.2}$$

and

$$\frac{1}{N}\sum_{j=1}^{N} Y_j^2 \approx \frac{\oint_{\text{unit circle}} Y^2 ds}{\oint_{\text{unit circle}} ds} = 1/2 \tag{6.3}$$

Consequently

$$\underline{L} \approx N \begin{bmatrix} 1/2 & 0 \\ 0 & 1/2 \end{bmatrix} \quad \underline{\Gamma} \approx \frac{1}{N}\begin{bmatrix} 2 & 0 \\ 0 & 2 \end{bmatrix} \tag{6.4}$$

Thus for example

$$\text{GDOP} \approx \left(\frac{2+2}{N}\right)^{1/2} = 2/\sqrt{N} \tag{6.5}$$

END OF EXAMPLE

Example 6.2 (Spherical Constellation): Consider a uniform spherical constellation of N beacons centered at the subject.

18-4-15150

The beacon images $P_1..P_N$ are uniformly distributed over the unit sphere as shown in Figure 6.2. Thus CM is at the center of the sphere.

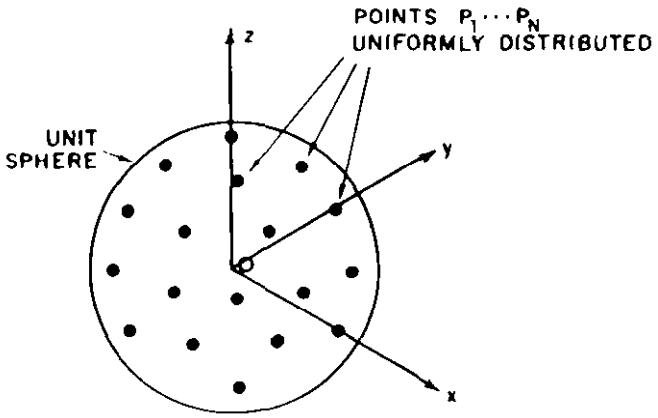

Figure 6.2

The $\underline{L}$ matrix is diagonal as a result of the symmetry of the points $P_1..P_N$. Moreover

$$\frac{1}{N}\sum_{j=1}^{N}(X_j)^2 = \frac{1}{N}\sum_{j=1}^{N}(Y_j)^2 = \frac{1}{N}\sum_{j=1}^{N}(Z_j)^2 \approx \frac{\oint X^2\, da}{\oint da}_{\text{unit sphere}} = \frac{1}{3} \tag{6.6}$$

Consequently

$$\underline{L} = N\begin{bmatrix} 1/3 & 0 & 0 \\ 0 & 1/3 & 0 \\ 0 & 0 & 1/3 \end{bmatrix}, \quad \underline{\Gamma} = \frac{1}{N}\begin{bmatrix} 3 & 0 & 0 \\ 0 & 3 & 0 \\ 0 & 0 & 3 \end{bmatrix} \tag{6.7,8}$$

Thus, for example,

$$\sigma_x \approx (\sigma_\tau c)\sqrt{3/N} \tag{6.9}$$

$$\text{GDOP} \approx \left(\frac{3+3+3}{N}\right)^{1/2} = 3/\sqrt{N} \tag{6.10}$$

END OF EXAMPLE

In some cases it simplifies calculations to determine the moments $\sum X^2$ etc. relative to some point other than the center of mass, and then translate the moments to the center of mass by using the "parallel axis theorem" of elementary mechanics. The translation step involves use of the relationships

$$\overline{X^2} = \overline{(X')^2} - (\overline{X'})^2 \quad , \quad \overline{XY} = \overline{X'Y'} - \overline{X'} \cdot \overline{Y'} \qquad (6.11,12)$$

$$\overline{Y^2} = \overline{(Y')^2} - (\overline{Y'})^2 \quad , \quad \overline{XZ} = \overline{X'Z'} - \overline{X'} \cdot \overline{Z'} \qquad (6.13,14)$$

$$\overline{Z^2} = \overline{(Z')^2} - (\overline{Z'})^2 \quad , \quad \overline{YZ} = \overline{Y'Z'} - \overline{Y'} \cdot \overline{Z'} \qquad (6.15,16)$$

where

X, Y, Z	denote coordinates measured in a cartesian coordinate system (X,Y,Z) set up at the center of mass
X', Y', Z'	denote coordinates measured in a second coordinate system (X', Y', Z') that differs from (X, Y, Z) by a translation
$\overline{\quad\quad}$	denotes the operation of averaging over the points $P_1, P_2, \ldots P_N$.

The following example is one where the parallel axis theorem proves useful.

Example 6.3 (Conical Constellation): Consider a constellation of N beacons uniformly distributed within a cone of half angle as shown in Figure 6.3.

The array of vectors $\underline{i}_1 .. \underline{i}_N$ and points $P_1 .. P_N$ is shown in Figure 6.4.

The basic computations required for $\underline{L}$ are most easily carried out in terms of a cartesian coordinate system X', Y', Z' centered at the origin O and having its Z' axis coincident with the cone axis as shown.

Straightforward calculation shows that

$$(X')^2 = (Y')^2 \approx \frac{\iint_S x^2 \, da}{\iint_S da} = \frac{\frac{\pi}{3}[2-3\cos\phi+\cos^2\phi]}{2\pi[1-\cos\phi]}$$

$$= \frac{(1-\cos\phi)(2+\cos\phi)}{6} \tag{6.17}$$

$$(Z')^2 \approx \frac{\iint_S z^2 \, da}{\iint_S da} = \frac{\frac{2}{3}\pi[1-\cos^3\phi]}{2\pi[1-\cos\phi]} = \frac{1+\cos\phi+\cos^2\phi}{3} \tag{6.18}$$

$$Z' \approx \frac{\iint_S z \, da}{\iint_S da} = \frac{1}{2}(1+\cos\phi) \tag{6.19}$$

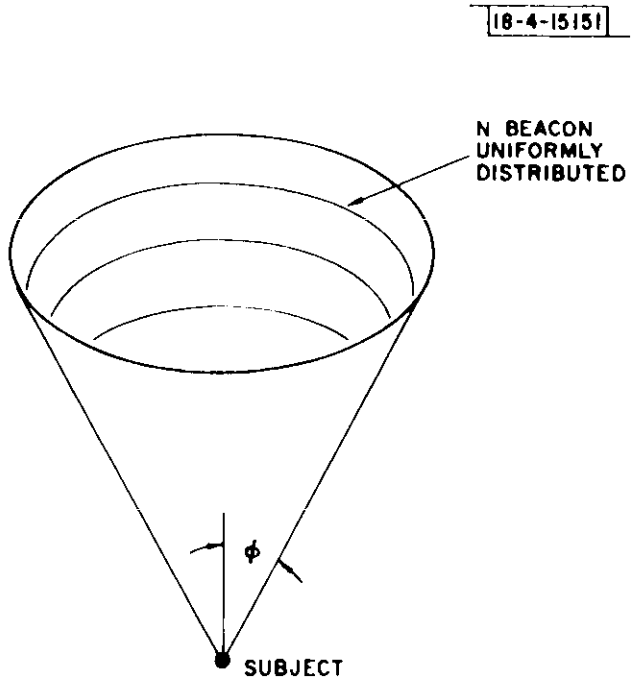

Figure 6.3

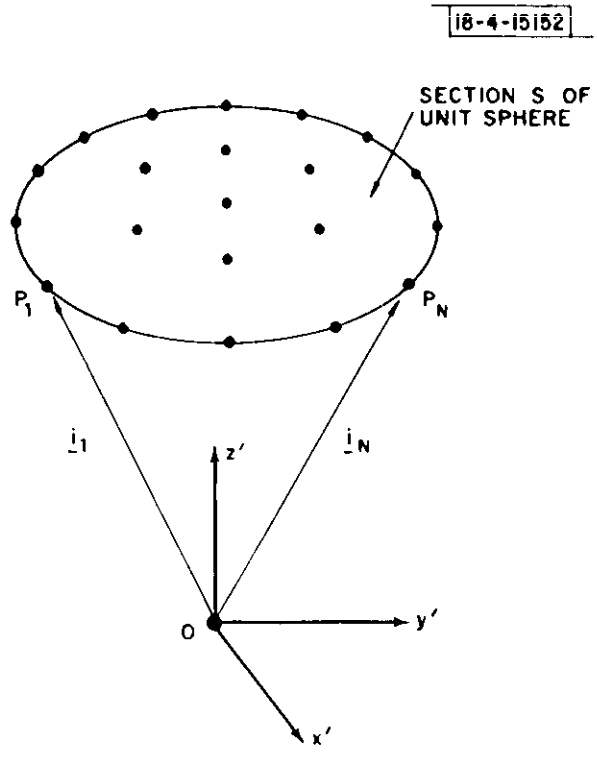

Figure 6.4

Moreover by symmetry

$$\overline{X'\,'} = \overline{X'\,'} = \overline{Y'\,'} = 0 \tag{6.20}$$

and

$$\overline{X'} = \overline{Y'} = 0$$

Equations (6.11-6.16) can be used to translate the moments (6.17), (6.18) and (6.20) to the center of mass. The results are:

$$\overline{X^2} = \overline{Y^2} = \frac{(1-\cos\phi)(2+\cos\phi)}{6} \tag{6.22}$$

$$\overline{Z^2} = \overline{(Z')^2} - (Z')^2 = \frac{(1-\cos\phi)^2}{12} \tag{6.23}$$

$$\overline{XY} = \overline{XY} = \overline{YZ} = 0 \tag{6.24}$$

Consequently the $\underline{L}$ and $\underline{\Gamma}$ matrices are:

$$\underline{L} \simeq N \begin{bmatrix} \frac{(1-\cos\phi)(2+\cos\phi)}{6} & 0 & 0 \\ 0 & \frac{(1-\cos\phi)(2+\cos\phi)}{6} & 0 \\ 0 & 0 & \frac{(1-\cos\phi)^2}{12} \end{bmatrix} \tag{6.25}$$

$$\underline{\Gamma} \quad \frac{1}{N} \begin{bmatrix} \frac{6}{(1-\cos\phi)(2+\cos\phi)} & 0 & 0 \\ 0 & \frac{6}{(1-\cos\phi)(2+\cos\phi)} & 0 \\ 0 & 0 & \frac{12}{(1-\cos\phi)^2} \end{bmatrix} \tag{6.26}$$

Thus for example the error measures σ_z^2 and GDOP are approximated as follows.

$$\sigma_z^2 \approx (\sigma_\tau c)^2 \frac{12}{N(1-\cos\phi)^2} \tag{6.27}$$

$$\text{GDOP} \approx \frac{1}{N} \left(\frac{2(6)}{(1-\cos\phi)(2+\cos\phi)} + \frac{12}{(1-\cos\phi)^2} \right)^{1/2}$$

$$= \sqrt{\frac{36}{N(1-\cos\phi)^2(2+\cos\phi)}} \tag{6.28}$$

END OF EXAMPLE

Note that GDOP $\to 0$ as $N \to \infty$ in each of Examples 6.1-6.3. This reflects the fact that the RMS positional error tends to zero when the results of a large number of uncorrelated measurements are averaged together to calculate position as described in Section III.

With regard to Example 6.3 it is interesting that GDOP $\to 0$ as $N \to \infty$ even for very small values of ϕ.

Many practical beacon constellations satisfy the conditions of Example 6.3; namely the constellations are (nearly) uniform and can be regarded as confined to a cone. Thus results like (6.26)-(6.28) are quite useful. The approximate $\underline{r}$ matrix (6.26) produces error measures that typically are accurate to 40% for moderate values of N. The next two examples show how the approximation (6.26) can be refined to produce error measures that typically are accurate to 2-5%.

Example 6.4: Consider the use of (6.28) to approximate the exact GDOP (5.24) for the beacon constellation shown in Figure 5.4.

Table 6.1 summarizes the values of (5.24) and (6.28) for typical values of ϕ.

Table 6.1

ϕ	Exact GDOP Eq. (5.24)	Approx. GDOP Eq. (6.28)
30°	8.92	13.2
45°	4.27	6.22
60°	2.67	3.79
90°	1.63	2.15

Clearly (6.28) approximates (5.24) to no better than 40%. Thus the assumption that the four mass points in Figure 5.4 can be well approximated by a uniform distribution of mass within the same area is not a particularly good one.

A method for improving the approximation (6.28) consists of "smearing out" the points $P_1..P_4$ on the unit sphere, and then using (6.28) to calculate GDOP. The "smeared out" counterparts of $P_1..P_4$ cover a larger portion of the unit sphere than the circle defined by the half angle ϕ. Thus the approach entails use of a cone angle ϕ' in (6.28) which is somewhat larger than the actual angle ϕ.

A suitable value of ϕ' can be obtained as follows. Spreading out $P_1..P_4$ radially and uniformly about their centers, causes half each of P_1, P_2, P_3 and all of P_4 to be within the circle ϕ. Therefore the density of points within the circle is

$$\text{Density} = \frac{3/2 + 1}{\text{area}}$$

$$= \frac{5/2}{2\pi\ (1-\cos\ \phi)} = \frac{5}{4\pi\ (1-\cos\ \phi)} \tag{6.29}$$

Thus the area consumed by all four points is

$$\text{Area} = \frac{\text{No. Points}}{\text{Density}}$$

$$= \frac{4}{5/4\pi\ (1-\cos\ \phi)} = \frac{16\pi}{5}\ (1-\cos\ \phi) \tag{6.30}$$

If this area is confined to the portion of the unit sphere defined by ϕ' [Area = $2\pi\ (1-\cos\ \phi')$] then ϕ' satisfies

$$2\ \pi(1-\cos\ \phi') = \frac{16\ \pi(1-\cos\ \phi)}{5} \tag{6.31}$$

or

$$\cos\ \phi' = 1 - \frac{8}{5}\ (1-\cos\ \phi) \tag{6.32}$$

Thus the result of "smearing out" $P_1..P_4$ is to approximate GDOP by

$$GDOP \approx \sqrt{\frac{36}{N(1-\cos\phi')^2(2+\cos\phi')}} \qquad (6.33)$$

where ϕ' is determined by Equation (6.32).

Equation (6.32) can be used to express the approximation (6.33) directly in terms of the cone half angle ϕ. Specifically substitution of (6.32) into (6.33) yields

$$GD \approx \sqrt{\frac{9\,(5/8)^3}{(1-\cos\phi)^2(\frac{7}{8}+\cos\phi)}} \qquad (6.34)$$

Table 6.2 compares the values of (5.24) and (6.34) for several values of ϕ.

Table 6.2

ϕ	Exact GDOP Eq. (5.24)	Approx. GDOP Eq. (6.34)
30°	8.92	8.38
45°	4.27	4.02
60°	2.67	2.53
90°	1.63	1.59

Clearly (6.34) provides an approximation to (5.24) accurate to within a few percent.

END OF EXAMPLE

Example 6.5: The basic approach used in Example 6.4 can be used to improve the more general approximation (6.26).

The reasoning leading to (6.31) in Example 6.4 shows that the exagerated cone angle ϕ' generally satisfies

$$2\pi\ (1-\cos\ \phi') = \frac{N}{N_i}\quad 2\pi\quad (1-\cos\ \phi) \tag{6.35}$$

or

$$\cos\ \phi' = 1\ -\ \frac{N}{N_i}\ (1-\cos\ \phi) \tag{6.36}$$

where N_i denotes the number of points $P_1..P_N$ remaining inside the circle after "smearing". Use of (6.36) in (6.26) with the latter evaluated at the exagerated cone angle ϕ' yields

$$\underline{r} \approx \frac{1}{N}\left(\frac{N_i}{N}\right)^2 \begin{bmatrix} \frac{6}{(1-\cos\ \phi)(A+\cos\ \phi)} & 0 & 0 \\ 0 & \frac{6}{(1-\cos\ \phi)(A+\cos\ \phi)} & 0 \\ 0 & 0 & \frac{12}{(1-\cos\ \phi)^2} \end{bmatrix} \tag{6.37}$$

where

$$A = 3\left(\frac{N_i}{N}\right) - 1. \tag{6.38}$$

It can be shown that the following expression is a good approximation to N_i

$$N_i \approx N + \frac{B}{2} - \sqrt{(N-1)\,B + \left(\frac{B}{2}\right)^2} \tag{6.39}$$

where

$$B = \pi \left[\frac{\sin \phi}{2 \sin \frac{\phi}{2}}\right]^2 \tag{6.40}$$

Thus (6.37)-(6.40) comprise an improved approximation to $\underline{\Gamma}$. Specifically Equations (6.38)-(6.40) are used to calculate A and N_i. The results then are used in (6.37) to calculate $\underline{\Gamma}$.

As an illustration consider the uniform 15 beacon constellation of Example 5.5. The exact $\underline{\Gamma}$ and GDOP are as follows.

$$\underline{\Gamma} = \begin{bmatrix} .182 & 0 & 0 \\ 0 & .182 & 0 \\ 0 & 0 & .463 \end{bmatrix} \tag{6.41}$$

$$\text{GDOP} = .910 \tag{6.42}$$

Moreover it is clear from Figure 5.6 that

$$N_i = 15 - \frac{8}{2} = 11. \tag{6.43}$$

By contrast use of (6.31)-(6.33) yields the following approximations

$$\underline{\Gamma} = \begin{bmatrix} .179 & 0 & 0 \\ 0 & .179 & 0 \\ 0 & 0 & .433 \end{bmatrix} \tag{6.44}$$

$$\text{GDOP} \approx .889 \tag{6.45}$$

$$N_i \approx 11.03 \tag{6.46}$$

Clearly the quantitives (6.44)-(6.46) approximate (6.41)-(6.43) to within 2-6%.

With regard to (6.38), (6.39) note that $N_i/N \to 1$ and $A \to 2$ as $N \to \infty$. Thus as one would expect, the refined error magnification matrix (6.37) approaches (6.26) as $N \to \infty$.

END OF EXAMPLE

VII. DEPENDENCY OF ACCURACY ON NUMBER OF BEACONS

Equations (4.7) and (4.9) for the inverse of the error magnification matrix $\underline{\Gamma}$ indicate that each additional beacon causes a new moment or product of inertia to be added to the elements of $\underline{L}$. This fact suggests successively that as the number N of beacons increases

1) the elements of $\underline{L}$ increase more or less in direct proportion to N

2) the elements of $\underline{\Gamma} = \underline{L}^{-1}$ decrease roughly in proportion to 1/N

3) the various measures of RMS error [e.g. $\sigma_x/(c\sigma_\tau) = (\Gamma_{xx})^{1/2}$, $GDOP = (\Gamma_{xx} + \Gamma_{yy} + \Gamma_{zz})^{1/2}$] decrease in proportion to $1/\sqrt{N}$

Examples 6.1-6.3, 6.5 confirm the foregoing hypothesis for the case of uniform beacon constellations. The results of Examples 6.1-6.3 show exactly the dependence described above. The (refined) results of Example 6.5 show substantially the same dependence, the only departure being the slow bounded growth of the quantities (N_i/N) and A.

Thus it is clear that for relatively uniform beacon constellations, the various error measures are not highly sensitive to the number of beacons. For example, to halve the RMS error measures it is necessary to increase the number of beacons by a factor of four.

The following example shows that the $1/\sqrt{N}$ dependence of RMS errors is not unique to uniform beacon constellations.

Example 7.1: Consider an arbitrary three dimensional constellation of N beacons. Let (x,y,z) denote any cartesian coordinate system at CM.

Clearly each mass image on the unit sphere has a moment arm not longer than the sphere diameter (i.e., 2). Thus

$$L_{xx} = \sum_{j=1}^{N} (x_j)^2 \leq \sum_{j=1}^{N} (2)^2 = 4N \qquad (7.1)$$

Similarly

$$L_{yy} \leq 4N \quad \text{and} \quad L_{zz} \leq 4N \tag{7.2,7.3}$$

Appendix I shows that each diagonal element of $\underline{\Gamma}$ satisfies the inequality

$$\Gamma_{\alpha\alpha} \geq \frac{1}{L_{\alpha\alpha}} \tag{7.4}$$

Use of (7.1)-(7.3) in (7.4) shows that

$$\Gamma_{xx} \geq \frac{1}{4N} \quad , \quad \Gamma_{yy} \geq \frac{1}{4N} \tag{7.5,7.6}$$

$$\Gamma_{zz} \geq \frac{1}{4N} \tag{7.7}$$

It follows that the RMS error measures σ_x, σ_y, σ_z, σ and GDOP are bounded from below as follows.*

$$\frac{\sigma_x}{(c\sigma_\tau)} \geq \frac{1}{2\sqrt{N}} \quad , \quad \frac{\sigma_y}{(c\sigma_\tau)} \geq \frac{1}{2\sqrt{N}} \tag{7.8,7.9}$$

$$\frac{\sigma_z}{(c\sigma_\tau)} \geq \frac{1}{2\sqrt{N}} \tag{7.10}$$

$$\frac{\sigma}{(c\sigma_\tau)} \geq \frac{\sqrt{3}}{2\sqrt{N}} \tag{7.12}$$

$$\text{GDOP} \geq \frac{\sqrt{3}}{2\sqrt{N}} \tag{7.12}$$

*By utilizing the result of Appendix II with $\phi = \pi$, the bounds (7.1)-(7.3) can be sharpened to $L_{\alpha\alpha} \leq N$. Thus the factor of 2 can be eliminated from the bounds (7.8)-(7.12).

Inequalities (7.8)-(7.12) show that the RMS error measures cannot decrease more rapidly than $1/\sqrt{N}$ as $N \to \infty$. For example, it is impossible for GDOP to have a $1/N$ dependence for large N.

END OF EXAMPLE

Additional constellations for which the RMS error measures exhibit an exact $1/\sqrt{N}$ dependence are given in Examples 10.1, 10.2, 11.3 and 11.4.

VIII. DEPENDENCE OF ACCURACY ON CONE ANGLE

In many three dimensional hyperbolic systems the visible beacons are confined to a "viewing cone". All accuracy measures normally are very sensitive to the half angle of the viewing cone.

The sensitivity of accuracy to the half angle ϕ of the viewing cone is apparent from Table 8.1. The table compares the actual angular dependence of GDOP for five different beacon constellations. All entries are normalized to unity at $\phi = 20°$. The quantity $GDOP_4$ denotes the (normalized) GDOP for the four beacon constellation treated in Example 5.4. The quantities $GDOP_{15}$ and $GDOP_{100}$ denote the GDOPs for uniform constellations containing respectively 15 and 100 beacons, calculated by the method of Example 6.5. GDOP denotes GDOP for the constellation of Example 6.3. $GDOP_{opt}$ denotes GDOP for an optimum beacon constellation treated in Example 10.2.

It is clear from the table that accuracy increases rapidly with increasing half cone angle. For example, increasing ϕ from 40° to 60° halves the rms error (i.e., GDOP) in all cases. Note that to obtain the same increase in accuracy by the expedient of adding beacons with $\phi = 40°$ it is necessary to increase the number of beacons by a factor of four (see Section VII).

The following example derives an approximate expression for accuracy (i.e., GDOP), and "explains" why accuracy is so dependent on ϕ.

TABLE 2.2

Numerical GDOPs

					$GDOP_{\infty}$	$GDOP_{opt}$
20°					1.000	1.000
30°					.265	.270
60°					.131	.137
90°					.073	.084

Example 8.1: Consider a rotationally symmetric constellation of N beacons confined to a cone of half angle ϕ.

The images $P_1..P_N$ of the beacons on the unit sphere are shown in Figure 8.1. Because of the rotational symmetry, the indicated coordinate system produces a diagonal $\underline{L}$ matrix.

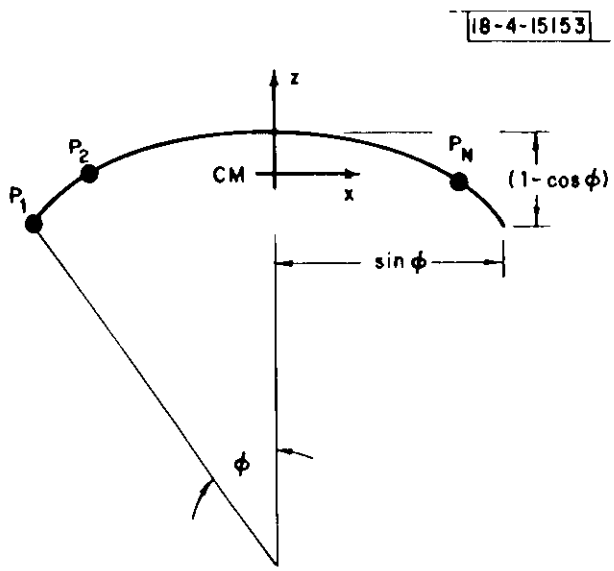

Figure 8.1

Clearly the mean moment arm in the x direction for the unit masses is roughly proportional to the x-extent of the spherical section. A reasonable estimate for the mean moment arm is $\phi/2$. Thus to a rough approximation

$$L_{xx} \approx N\,(\phi/2)^2 \tag{8.1}$$

By symmetry

$$L_{yy} \approx N\,(\phi/2)^2 \tag{8.2}$$

Similarly the mean moment arm in the z direction for the unit masses is roughly proportional to the z extent of the spherical section. A reasonable estimate of the z directed moment arm is $\frac{1}{\sqrt{2}}\left(\frac{1-\cos\phi}{2}\right) \approx \phi^2/4\sqrt{2}$. Consequently

$$L_{zz} \approx N(\phi^2/4\sqrt{2})^2 = N\phi^4/32 \tag{8.3}$$

Thus to a rough approximation

$$\underline{L} \approx N \begin{bmatrix} \phi^2/4 & 0 & 0 \\ 0 & \phi^2/4 & 0 \\ 0 & 0 & \phi^4/32 \end{bmatrix} \tag{8.4}$$

$$\underline{\Gamma} = \underline{L}^{-1} \approx \frac{1}{N} \begin{bmatrix} 4/\phi^2 & 0 & 0 \\ 0 & 4/\phi^2 & 0 \\ 0 & 0 & 32/\phi^4 \end{bmatrix} \tag{8.5}$$

Equation (8.5) indicates that the RMS error measures depend upon angle approximately as follows

$$\sigma_x/(c\sigma_\tau) \approx K_1/\phi \qquad \sigma_y/(c\sigma_\tau) \approx K_1/\phi \tag{8.6,8.7}$$

$$\sigma_z/(c\sigma_\tau) \approx K_2/\phi \tag{8.8}$$

$$\sigma/(c\sigma_\tau) \approx K_3\,(1/\phi^2 + 4/\phi^4)^{1/2} \tag{8.9}$$

$$\text{GDOP} \approx K_3\,(1/\phi^2 + 4/\phi^4)^{1/2} \tag{8.10}$$

An indication of the quality of approximations (8.6)-(8.10) can be obtained by comparing the angular dependence of GDOP predicted by (8.10) with that exhibited by the constellations previously considered. Reference to Table (8.1) shows that the angular dependence predicted by (8.10) is quite reasonable considering the coarseness of approximations (8.1)-(8.3).

END OF EXAMPLE

IX. DEPENDENCE OF ACCURACY ON DIRECTION

The errors that result from the minimum squared error estimate of position (3.7) have a distinct directional dependence if the beacons are confined to a relatively narrow sector or cone. Specifically errors in the direction of the sector or cone axis dominate. This means that in many three dimensional systems altitude errors dominate.

The following two dimensional example explains why this is the case.

Example 9.1: *Consider a constellation of N beacons confined to a* sector of half angle ϕ. Assume that the beacons are positioned so that the center of mass CM falls on the vertical centerline as as shown in Figure 9.1.

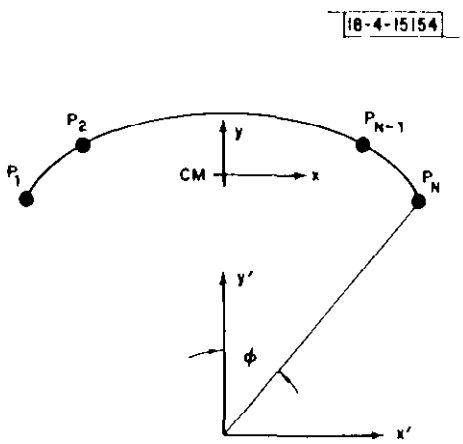

Figure 9.1

Note that the x extent of the arc greatly exceeds the Y extent of the arc. This suggests that

$$\sum_{i=1}^{N} x_i^2 >> \sum_{i=1}^{N} y_i^2 \tag{9.1}$$

or

$$L_{xx} >> L_{yy} \tag{9.2}$$

so that

$$\frac{\sigma_y}{\sigma_x} = \sqrt{\frac{\Gamma_{yy}}{\Gamma_{xx}}} = \sqrt{\frac{L_{xx}}{L_{yy}}} \tag{9.3}$$

$$> \quad 1$$

In Appendix III it is shown that

$$\frac{L_{xx}}{L_{yy}} > \tan^2\left(\frac{\pi}{2} - \frac{\phi}{2}\right) \tag{9.4}$$

so that

$$\frac{\sigma_y}{\sigma_x} > \tan\left(\frac{\pi}{2} - \frac{\phi}{2}\right) \tag{9.5}$$

Thus it is clear from (9.5) that $\sigma_y/\sigma_x > 1$ whenever $\phi < \pi/2$.

For $\phi = 45°$, (9.5) shows that

$$\frac{\sigma_y}{\sigma_x} > \tan 67.5° = 2.41 \tag{9.6}$$

The construction of Figure 9.2 provides a simple intrepretation of the condition (9.5). In particular the ratio σ_y/σ_x exceeds the ratio b/a shown in the figure.

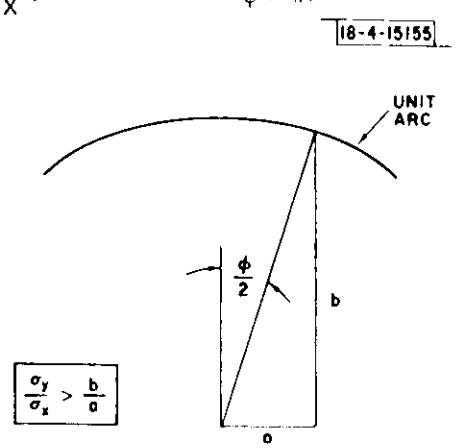

Figure 9.2

END OF EXAMPLE

An entirely analoagous situation obtains for three dimensional constellations confined to a cone. That is, errors in the direction of the cone axis (or altitude errors) dominate. The following examples illustrate this point.

Example 9.2: Consider a constellation of 20 beacons uniformly distributed within a cone having half angle ϕ. Let (X,Y,Z) denote a coordinate system origined at the center of mass of points $P_1, P_2, \ldots P_N$, and oriented so that the Z axis coincides with the cone axis.

The ratios L_{zz}/L_{xx}, σ_z/σ_x and σ_z/σ_y can be calculated for different cone angles using the result of Example 6.5. Results for a representative set of angles are given in Table 9.1.

Table 9.1

ϕ	$\frac{L_{zz}}{L_{xx}} = \frac{L_{zz}}{L_{yy}}$	$\frac{\sigma_z}{\sigma_x} = \sqrt{\frac{\Gamma_{zz}}{\Gamma_{xx}}} = \sqrt{\frac{L_{xx}}{L_{zz}}}$	$\frac{\sigma_z}{\sigma}$
1°	3.71×10^{-5}	164.19	.9999
30°	.0344	5.38	.97
45°	.0806	3.52	.93
60°	.1508	2.57	.88
90°	.387	1.61	.75

Note that errors in the z direction dominate for cone angles less than 90°. For angles typical of synchronous satellite constellations (i.e., 45°-60°) L_{xx} is an order of magnitude larger than L_{zz}, and σ_z exceeds σ_x by a factor of 3 so that total rms error σ is due almost entirely to rms error in the z direction.

END OF EXAMPLE

Example 9.3: The results of Example 9.1 can easily be extended to the case of three dimensional beacon constellations confined to a cone.

Specifically a bound analogous to (9.5) applicable to three dimensional constellations is derived in Appendix III. The bound is as follows.

$$\frac{\sigma_z^2}{\sigma_x^2} + \frac{\sigma_z^2}{\sigma_y^2} \geq \tan^2\left(\frac{\pi}{2} - \frac{\phi}{2}\right) \tag{9.7}$$

The bound is applicable to any constellation of N beacons confined to a cone of half angle ϕ, provided that the center of mass CM of points $P_1, P_2, \ldots P_N$ lies on the cone axis. The X,Y,Z axes are assumed to be centered at CM and oriented so that the Z axis coincides with the cone axis, and so that $L_{xy} = 0$.

In the case of a constellation rotationally symmetric about the cone axis $\sigma_x^2 = \sigma_y^2$ so that (9.7) reduces to

$$\frac{\sigma_z^2}{\sigma_x^2} \geq \frac{1}{2} \tan^2\left(\frac{\pi}{2} - \frac{\phi}{2}\right) \tag{9.8}$$

which implies

$$\frac{\sigma_z}{\sigma_x} \geq \tan\left(\frac{\pi}{2} - \frac{\phi}{\sqrt{2}}\right) \tag{9.9}$$

Inequality (9.8) shows that $\sigma_z/\sigma_y > 1$ whenever

$$\frac{1}{\sqrt{2}} \tan\left(\frac{\pi}{2} - \frac{\phi}{2}\right) > 1 \tag{9.10}$$

or

$$\phi \leq 70.6° \tag{9.11}$$

Note that the interpretation of Figure 9.2 is directly applicable to condition (9.9) if $\phi/2$ is replaced by $\phi/\sqrt{2}$ and Y is replaced by Z.

END OF EXAMPLE

The dominance of altitude errors is unfortunate from the point of view of aircraft surveillance systems that rely entirely upon satellite beacons. In such system it is desirable to know altitude more accurately than transverse position. The results of this section show that the opposite is the case.

X. ERROR MINIMIZATION I

The following questions appear to be basic ones from the viewpoint of designing hyperbolic systems.

1) What is the minimum error that can be achieved from a given number of beacons?

2) How should the beacons be deployed to achieve minimum error?

This section and the following one answer questions of this kind.

Two error measures appear to be appropriate for hyperbolic systems. These measures are as follows.

1) The mean squared axial errors for beacon constellations restricted to a planar sector or to a cone; i.e., σ_z^2

2) The total mean squared error; i.e., $\sigma_x^2 + \sigma_y^2 + \sigma_z^2$ (equivalent to GDOP)

The present section identifies constellations that minimize mean squared axial error for constellations restricted to a planar sector, and to a cone. The following section identifies beacon constellations that minimize total mean squared error for four geometries of interest.

In all cases bounding arguments are used to identify the minimum mean squared error. This is, a lower bound on the mean squared error is established. Then it is shown that certain select constellations achieve the bound.

With respect to the first error measure, let α denote a coordinate axis parallel to the sector or cone axis of interest. The mean squared error σ_α^2 in the α direction is given by

$$\sigma_\alpha^2 = (\sigma_\tau c)^2 \, \Gamma_{\alpha\alpha} \tag{10.1}$$

where σ_τ and c are as in Section III, and $\Gamma_{\alpha\alpha}$ is the α-α element of the matrix $\underline{\Gamma}$. Clearly to minimize (10.1) it is necessary to minimize the magnification factor

$$\frac{\sigma_\alpha^2}{(\sigma_\tau c)^2} = \Gamma_{\alpha\alpha} \tag{10.2}$$

The following bound* is used as the starting point in the examples of the present section

$$\Gamma_{\alpha\alpha} \geq \frac{1}{L_{\alpha\alpha}} \tag{10.3}$$

where the equal sign holds if and only if $L_{\alpha\beta} = 0$ for $\beta \neq \alpha$. The bound is useful in that it facilitates use of coordinate systems with one axis parallel to the sector or cone axis rather than coordinate systems that diagonalize the $\underline{L}$ matrix.

The examples employ the "$\overline{\quad}$" notation to denote averaging over the set of points $P_1, P_2, \ldots P_N$; e.g., $\overline{Y^2} = \frac{1}{N}\sum_{j=1}^{N} (Y_j)^2$.

Example 10.1 (Planar Sector) Consider the problem of placing N beacons on a plane within a sector of half angle ϕ so as to minimize the axial squared error.

18-4-15156

Let C denote an arbitrary constellation of N beacons confined to the sector. Let the coordinate system (X,Y) be selected at the CM of the beacon images $P_1 .. P_N$ with the Y axis parallel to the sector axis as shown in

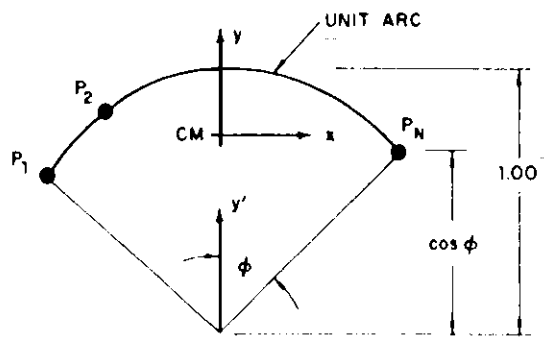

Figure 10.1

*See Appendix I

Figure 10.1. Let (X',Y') denote a parallel coordinate system at the center of the unit circle as shown. Let $\bar{Y}'$ denote the Y' coordinates of the CM in the system (X',Y').

It follows from (10.2), (10.3) that the mean square axial error σ_y^2 satisfies

$$\frac{\sigma_y^2}{(c\sigma_\tau)^2} \geq \frac{1}{L_{yy}} = \frac{1}{N\bar{Y}^2} \tag{10.4}$$

Intuition suggests that the denominator $\overline{NY^2}$ of (10.4) can be increased by removing the points $P_1,P_2,\ldots P_N$ from the center of mass $\bar{Y}'$ as far as possible while maintaining $\bar{Y}'$. Appendix II shows that this is the case, and that the enhanced value of $\overline{Y^2}$ is $(1-\bar{Y}')(\bar{Y}'-\cos\phi)$. More precisely Appendix II shows that

$$\overline{Y^2} \leq (1-\bar{Y}')(\bar{Y}'-\cos\phi) \tag{10.5}$$

with equality holding if and only if $P_1,P_2,\ldots P_N$ are distributed between the minimum Y and maximum Y positions of the unit arc as shown in Figure 10.2. Use of (10.5) in (10.4) shows that

$$\frac{\sigma_y^2}{(c\sigma_\tau)^2} \geq \frac{1}{N}\,\frac{1}{(1-\bar{Y}')(\bar{Y}'-\cos\phi)} \tag{10.6}$$

Thus to find the minimizing constellation it is only

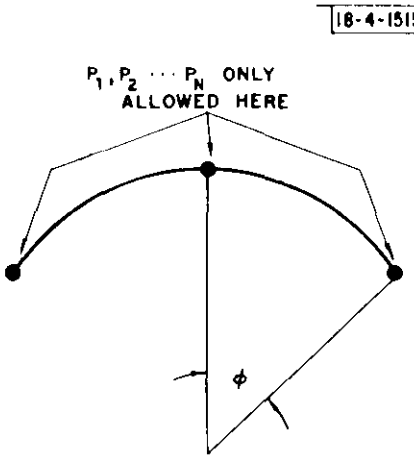

Figure 10.2

necessary to examine all constellations of the type shown in Figure.10.2, and select the one that minimizes σ_y^2. That is,

$$\frac{\sigma_y^2}{(c\sigma_\tau)^2} \geq \frac{1}{N} \underset{\cos\phi \leq \overline{Y'} \leq 1}{\text{Minimum}} \left\{ \frac{1}{(1-\overline{Y'})(\overline{Y'}-\cos\phi)} \right\}$$

$$= \frac{1}{N} \frac{1}{\sin^4 \frac{\phi}{2}} . \qquad (10.7)$$

The minimizing calculation shows that the minimum is obtained for $\overline{Y'}$ equidistant between the limits $\cos\phi$ and 1.

A straightforward calculation shows that any constellation of the type shown in Figure 10.3 achieves the bound (10.7) provided

$$N_1 = N/2 \qquad (10.8)$$

$$N_2 + N_3 = N/2. \qquad (10.9)$$

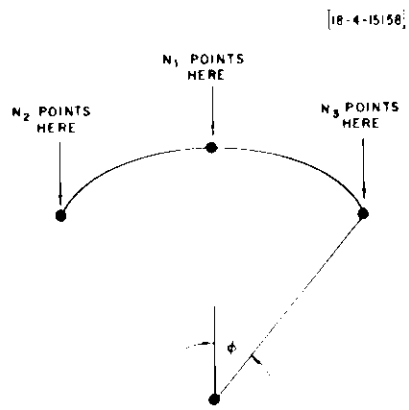

Figure 10.3

Moreover a careful review of the inequalities (10.4)-(10.7) shows that these constellations are the only ones that achieve the bound (10.7).

Thus the minimizing constellation is that shown in Figure 10.3 with (10.8), (10.9) satisfied. The corresponding squared error is given by

$$\sigma_y^2 = (c\sigma_\tau)^2 \frac{1}{N} \frac{1}{\sin^4 \frac{\phi}{2}} \qquad (10.10)$$

END OF EXAMPLE

Example 10.2 Consider the problem of placing N beacons within a cone of half angle ϕ so as to minimize mean squared axial error at the vertex of the cone.

Let C denote an arbitrary constellation of N satellites confined to the cone. The system of vectors $\underline{i}_1, \underline{i}_2 \ldots \underline{i}_N$ and points $P_1, P_2 \ldots P_N$ are shown in Figure 10.4. Let the coordinate system (X,Y,Z) be set up at the center of mass CM so that the Z axis is parallel with the cone axis as shown.

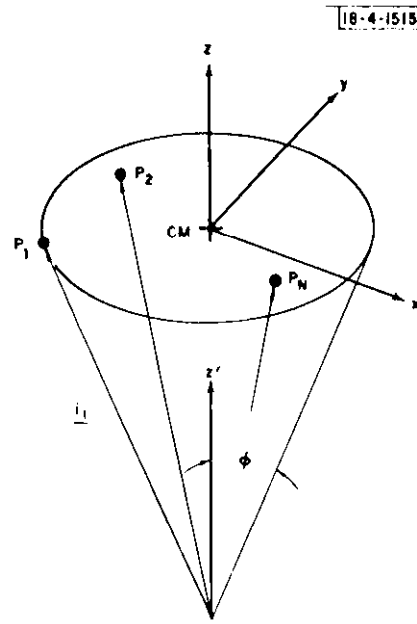

Figure 10.4

It follows from (10.2), (10.3) that

$$\frac{\sigma_z^2}{(c\sigma_\tau)^2} \geq \frac{1}{L_{zz}} = \frac{1}{N\bar{Z}^2} \tag{10.11}$$

The argument leading from (10.4) to (10.7) applies once again. Consequently

$$\frac{\sigma_z^2}{(c\sigma_\tau)^2} \geq \frac{1}{N} \quad \frac{1}{\sin^4 \frac{\phi}{2}} \tag{10.12}$$

with equality holding only if the beacons are distributed equally between the pole and ring as shown in Figure 10.5.

A straightforward calculation shows that the constellation of Figure 10.5 indeed achieves the bound (10.12) provided

$$N_1 = N_2 = N/2 \qquad (10.13)$$

Thus the minimizing constellation is that shown in Figure 10.5 with $N_1=N_2=N/2$. The corresponding minimum value of σ_z^2 is

$$\sigma_z^2 = (c\sigma_\tau)^2 \frac{1}{N} \frac{1}{\sin^4 \frac{\phi}{2}} \qquad (10.14)$$

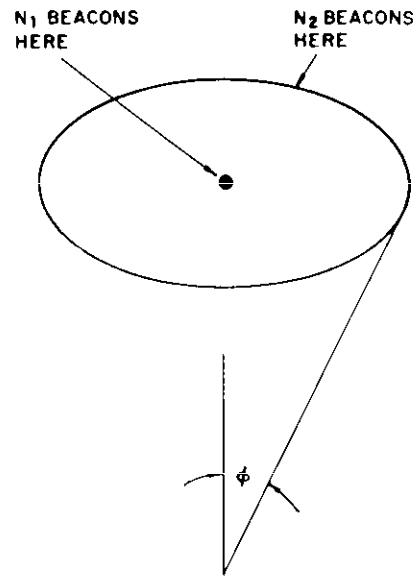

Figure 10.5

The minimum value of σ_z^2 given by (10.14) represents a clear improvement over that for a uniform constellation. As an illustration, consider the uniform fifteen beacon constellation shown in Figure 5.6. Example 5.5 shows that

$$\sigma_z^2/(c\sigma_\tau)^2 = .463 \qquad (10.15)$$

By contrast an optimum fifteen beacon constellation for the same half cone angle ($\phi=\pi/2$) exhibits the following mean squared error

$$\frac{\sigma_z^2}{(c\sigma_\tau)^2} = \frac{1}{15} \frac{1}{\sin^4 \frac{\pi}{4}} \qquad (10.16)$$

$$= .266$$

END OF EXAMPLE

XI. ERROR MINIMIZATION II

This section identifies beacon constellations that minimize total mean squared error (σ^2) or, equivalently GDOP. Four different beacon geometries are treated:

i) unconstrained two dimensional constellations
ii) unconstrained three dimensional constellations
iii) two dimensional constellations confined to a sector
iv) three dimensional constellations confined to a cone

The total mean squared error σ^2 is given by the sum of the diagonal elements of the covariance matrix (3.11). That is,

two dimensions:

$$\sigma^2 = (c\sigma_\tau)^2(\Gamma_{xx} + \Gamma_{yy}) \tag{11.1}$$

three dimensions:

$$\sigma^2 = (c\sigma_\tau)^2 (\Gamma_{xx} + \Gamma_{yy} + \Gamma_{zz})$$

Thus the quantity σ^2 is minimized by minimizing the magnification factors in (11.1); namely

two dimensions:

$$\sigma^2/(\sigma_\tau c)^2 = \Gamma_{xx} + \Gamma_{yy} \tag{11.2}$$

three dimensions

$$\sigma^2/(\sigma_\tau c)^2 = \Gamma_{xx} + \Gamma_{yy} + \Gamma_{zz}$$

The following bound* is used as a starting point in each example

two dimensions:

$$\Gamma_{xx} + \Gamma_{yy} \geq \frac{1}{L_{xx}} + \frac{1}{L_{yy}} \tag{11.3}$$

three dimensions:

$$\Gamma_{xx} + \Gamma_{yy} + \Gamma_{zz} \geq \frac{1}{L_{xx}} + \frac{1}{L_{yy}} + \frac{1}{L_{zz}} \tag{11.4}$$

where the equal sign applies if and only if $\underline{L}$ is diagonal. The bound is useful in that it facilitates use of coordinate systems that do not necessarily diagonalize $\underline{L}$.

The examples employ the following notation.

1) X', Y' (or X',Y',Z' in three dimensional examples) are cartesian coordinates measured with respect to the origin 0 of the system of unit vectors $\underline{i}_1, \underline{i}_2, \ldots \underline{i}_N$.

2) X, Y (or X,Y,Z in three dimensional examples) are cartesian coordinates measured with respect to the center of mass of the points $P_1, P_2, \ldots P_N$. It is assumed that the coordinate system X,Y (or X,Y,Z) differs from X',Y' (or X', Y',Z') by a translation so that Equations (6.11)-(6.16) can be used.

3) The "——" notation again is used to denote averaging over the set of points $P_1, P_2, \ldots P_N$.

Example 11.1 (Unconstrained Planar Constellation): Consider the problem of positioning N beacons in a plane so as to minimize the total mean squared error σ^2 at a point in the plane.

*see Appendix I

Let C denote any constellation of beacons in the plane. According to (11.2), (11.3)

$$\frac{\sigma^2}{(c\sigma_\tau)^2} \geq \frac{1}{L_{xx}} + \frac{1}{L_{yy}} \tag{11.5}$$

It follows from (4.10), (6.11) and (6.13) that the diagonal elements of $\underline{L}$ are given by

$$L_{xx} = N(\overline{X^2}) = N\left[\overline{(X')^2} - (\overline{X'})^2\right] \geq 0 \tag{11.6}$$

$$L_{yy} = N(\overline{Y^2}) = N\left[\overline{(Y')^2} - (\overline{Y'})^2\right] \geq 0 \tag{11.7}$$

Moreover geometry imposes the constraint

$$\overline{(X')^2} + \overline{(Y')^2} = 1 \tag{11.8}$$

since $(X_i')^2 + (Y_i')^2 = 1$ for each point P_i on the unit circle. Thus the bound (11.5) can be rewritten

$$\frac{\sigma^2}{(c\sigma_\tau)^2} \geq \frac{1}{N}\left[\frac{1}{\overline{X^2}} + \frac{1}{\overline{Y^2}}\right]$$

$$= \frac{1}{N}\left[\frac{1}{\overline{(X')^2} - (\overline{X'})^2} + \frac{1}{\overline{Y^2}}\right]$$

$$= \frac{1}{N}\left[\frac{1}{1-\overline{(Y')^2} - (\overline{X'})^2} + \frac{1}{\overline{Y^2}}\right] \tag{11.9}$$

$$= \frac{1}{N}\left[\frac{1}{1-\overline{(Y')^2} - (\overline{X'})^2} + \frac{1}{\overline{(Y')^2} - (\overline{Y'})^2}\right] \tag{11.10}$$

The denominators in (11.10) are bounded by

$$1-\overline{(Y')^2} \geq 1-\overline{(Y')^2} - \overline{(X')}^2 \geq 0 \tag{11.11}$$

$$\overline{(Y')^2} \geq \overline{(Y')^2} - \overline{(Y')}^2 \geq 0 \tag{11.12}$$

Consequently

$$\frac{\sigma^2}{(c\sigma_\tau)^2} \geq \frac{1}{N}\left[\frac{1}{1-\overline{(Y')^2} - (\overline{X'})^2} + \frac{1}{\overline{(Y')^2} - (\overline{Y'})^2}\right] \tag{11.13}$$

$$\geq \frac{1}{N}\left[\frac{1}{1-\overline{(Y')^2}} + \frac{1}{\overline{(Y')^2}}\right]$$

$$\geq \frac{1}{N} \underset{0<\gamma<1}{\text{Min.}} \left[\frac{1}{1-\gamma} + \frac{1}{\gamma}\right]$$

$$= 4/N \tag{11.14}$$

where equality holds if and only if

$$\underline{L} = \text{diagonal} \tag{11.15}$$

$$\overline{X'} = \overline{Y'} = 0 \tag{11.16}$$

$$\overline{(X')^2} = \overline{(Y')^2} = 1/2 \tag{11.17}$$

It is easy to demonstrate constellations of N beacons that achieve the lower bound (11.14). Thus the bound represents the minimum value of $\sigma^2/(c\sigma_\tau)^2$. It follows that the minimum mean squared error is

$$\sigma^2_{\text{min}} = (c\sigma_\tau)^2 \; 4/N \tag{11.18}$$

The corresponding value for GDOP is

$$GDOP_{min} = 2/\sqrt{N} \tag{11.19}$$

Moreover Equations (11.15), (11.16) and (11.17) represent necessary and sufficient conditions for a beacon configuration to minimize σ^2.

The constellations considered in Examples 5.2 and 5.1 are examples of minimizing (or optimum) constellations for N=3 and N=4. More generally it can be shown that a constellation consisting of N beacons separated by 360°/N in azimuth is optimum.

It should be noted that beacon constellations other than "equally spaced" constellations also satisfy (11.15-11.17) and therefore are optimum. For example it is easy to show that superposition of the optimum N=3 and N=4 constellations considered in Examples 5.2 and 5.1 produces an optimum (non-equally spaced) constellation for N=7.

END OF EXAMPLE

Example 11.2 (Unconstrainted Three Dimensional Constellation): An analysis similar to that of Example 11.1 shows that for a 3 dimensional constellation of N beacons

$$\sigma^2 \geq (c_{\sigma_\tau})^2 \ 9/N \tag{11.20}$$

and

$$GDOP \geq 3/\sqrt{N} \tag{11.21}$$

Moreover equality in (11.20), (11.21) holds if and only if

$$L = \text{diagonal} \tag{11.22}$$

$$\bar{X}' = \bar{Y}' = \bar{Z}' = 0 \tag{11.23}$$

$$\overline{(X')^2} = \overline{(Y')^2} = \overline{(Z')^2} = 1/3 \tag{11.24}$$

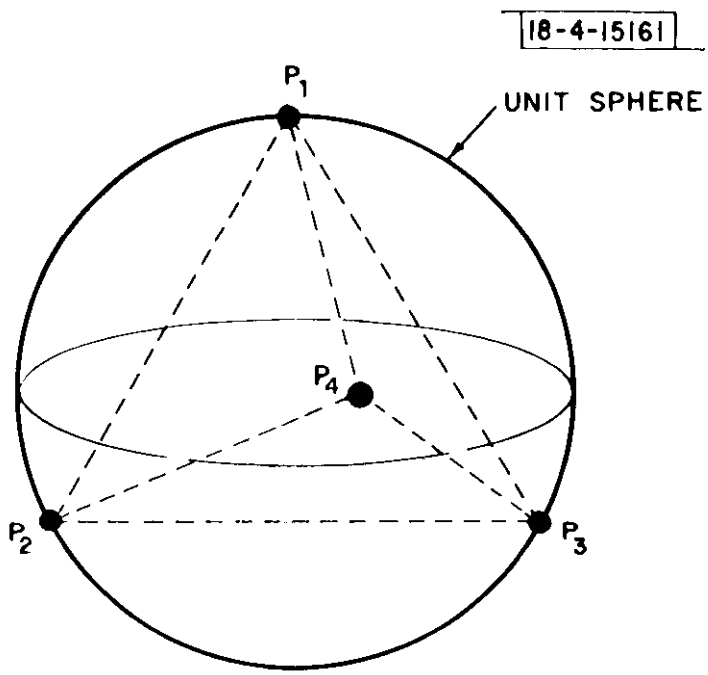

Figure 11.1

It is easy to show that the minimizing conditions (11.22-11.24) are satisfied for N=4, 6, 8 if the points $P_1, P_2, \ldots P_N$ are placed at the vertices of the appropriate regular solid inscribed within the the unit sphere. For example, the "tetrahedral" constellation in Figure 11.1 satisfies (11.22-11.24). Furthermore the results of Example 6.2 show that the minimizing conditions are approximately satisfied for any value of N, if P_1, $P_2 \ldots P_N$ are "uniformly distributed" over the unit sphere.

Consequently (11.20) and (11.21) represent the minimum values of σ^2 and GDOP for N=4, 6 and 8. For other values of N (11.20) and (11.21) can be regarded as lower bounds which are very nearly realized by uniform distributions of beacons.

Once again uniformly distributed constellations of beacons are not the only constellations that satisfy (11.22-11.24). For example it is easy to show that superimposing the (uniform) optimum constellations for N=4 and N=8 produces an optimum (but non-uniform) constellation for N=12.

END OF EXAMPLE

Example 11.3 (Planar Sector Configuration): Consider the problem of placing N beacons on a plane within a sector of half angle ϕ so as to minimize total mean squared error σ^2 at the vertex of the sector.

Let C denote a constellation of N beacons confined to the sector. The system of vectors $\underline{i}_1, \underline{i}_2, \ldots \underline{i}_N$ is shown in Figure 11.2. Let the coordinate system (X',Y') be selected as shown.

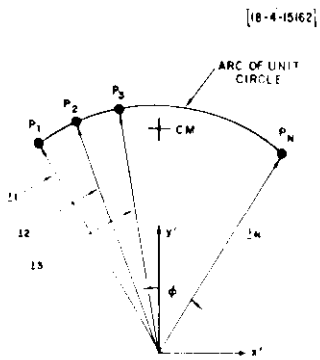

Figure 11.2

The reasoning leading to the bound (11.9) again is applicable. Consequently

$$\frac{\sigma^2}{(c\sigma_\tau)^2} \geq \frac{1}{N}\left[\frac{1}{1-(\overline{Y'})^2-(\overline{X'})^2} + \frac{1}{\overline{Y^2}}\right]$$

$$= \frac{1}{N}\left[\frac{1}{1-\overline{Y^2}-(\overline{Y'})^2-(\overline{X'})^2} + \frac{1}{\overline{Y^2}}\right]$$

$$\geq \frac{1}{N}\left[\frac{1}{1-\overline{Y^2}-(\overline{Y'})^2} + \frac{1}{\overline{Y^2}}\right] \qquad (11.25)$$

where equality in (11.25) applies only if $X' = 0$, and $\underline{L}$ is diagonal. As discussed in Example 10.1, $\overline{Y^2}$ satisfies the inequality

$$\overline{Y^2} \leq (1-\overline{Y'})(\overline{Y'}-\cos\phi) \qquad (11.26)$$

with the equal sign applying only if the points $P_1, P_2, \ldots P_N$ are confined to the minimum Y' and maximum Y' position of the unit are as shown in Figure 11.3. Given that $\overline{Y'} \leq 1$, it is a simple exercise to deduce from (11.26) that there exists an angle ϕ' satisfying

$$0 \leq \phi' \leq \phi \qquad (11.27)$$

such that*

$$\overline{Y^2} = (1-\overline{Y'})(\overline{Y'}-\cos\phi') \qquad (11.28)$$

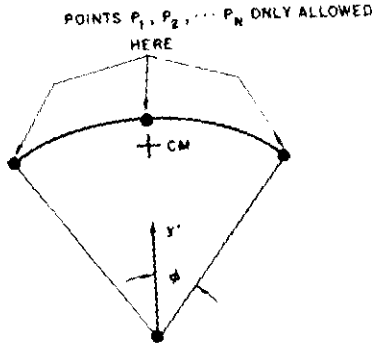

Figure 11.3

*See Appendix IV for an interpretation of (11.27) and of the subsequent inequality manipulations that lead to the final bound (11.33-11.34).

Consequently (11.25) can be rewritten

$$\frac{\sigma^2}{(c\sigma_\tau)^2} \geq \frac{1}{N}\left[\frac{1}{1-(1-\overline{\gamma}^\Gamma)(\overline{\gamma}^\Gamma-\cos\phi')-(\overline{\gamma}^\Gamma)^2} + \frac{1}{(1-\overline{\gamma}^\Gamma)(\overline{\gamma}^\Gamma-\cos\phi')}\right]$$

$$= \frac{1}{N}\left[\frac{1}{(1+\cos\phi')(1-\overline{\gamma}^\Gamma)} + \frac{1}{(\overline{\gamma}^\Gamma-\cos\phi')(1-\overline{\gamma}^\Gamma)}\right] \qquad (11.29)$$

It follows straightforwardly from (11.29) that

$$\frac{\sigma^2}{(c\sigma_\tau)^2} \geq \frac{1}{N} \underset{\cos\phi'\leq\overline{\gamma}^\Gamma\leq 1}{\text{Minimum}} \left\{\frac{1}{(1+\cos\phi')(1-\overline{\gamma}^\Gamma)} + \frac{1}{(\overline{\gamma}^\Gamma-\cos\phi')(1-\overline{\gamma}^\Gamma)}\right\} \qquad (11.30)$$

$$= \frac{1}{N} \frac{1}{16\cos^2\frac{\phi'}{2}\sin^4\frac{\phi'}{4}} \qquad (11.31)$$

$$\geq \frac{1}{N} \underset{0\leq\phi'\leq\phi}{\text{Minimum}} \left\{\frac{1}{16\cos^2\frac{\phi'}{2}\sin^4\frac{\phi'}{2}}\right\} \qquad (11.32)$$

$$= \begin{cases} \frac{1}{N} \dfrac{1}{16\cos^2\frac{\phi}{2}\sin^4\frac{\phi}{4}} & \text{for } \phi \leq \frac{2\pi}{3} \qquad (11.33) \\ \frac{4}{N} & \text{for } \phi > \frac{2\pi}{3} \qquad (11.34) \end{cases}$$

For $\phi \leq 2\pi/3$ the constellation $C^*(\phi)$ of points $P_1, P_2, \ldots P_N$ shown in Figure 11.4 achieves the lower bound (11.33) provided

$$N_1 = N\left[1-2\left(\frac{\sin\phi/4}{\sin\phi/2}\right)^2\right] \qquad (11.35)$$

$$N_2 = N_3 = N\left(\frac{\sin\phi/4}{\sin\phi/2}\right)^2 \qquad (11.36)$$

[18-4-15164]

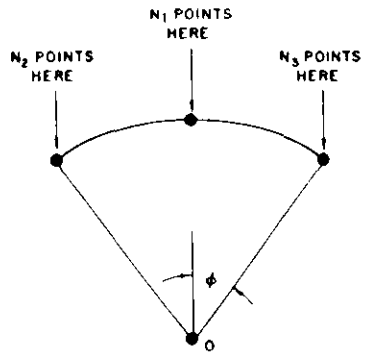

Figure 11.4

Moreover a careful review of the inequalities (11.25-11.33) shows that $C^*(\theta)$ is the only constellation that does achieve the bound.

Thus for $\phi \leq 2\pi/3$ the minimum squared error is

$$\sigma^2_{min} = (c\sigma_\tau)^2 \frac{1}{N} \frac{1}{16 \cos^2 \frac{\phi}{2} \sin^4 \frac{\phi}{4}} \tag{11.37}$$

The corresponding value of GDOP is

$$GDOP_{min} = \frac{1}{\sqrt{N}} \frac{1}{4 \cos \frac{\phi}{2} \sin^2 \frac{\phi}{4}} . \tag{11.38}$$

The minimizing constellation is that shown in Figure 11.4.

For $\phi \geq 2\pi/3$ any optimum constellation of Example 11.1 that is consistent with the sector constraint achieves the bound (11.34). For example the "equal angle" constellation shown in Figure 5.2, and multiples of it, achieves the bound (11.34).

Thus for $\phi > 2\pi/3$

$$\sigma^2_{min} = (c\sigma_\tau)^2 \ 4/N \tag{11.39}$$

and

$$GDOP_{min} = 2/\sqrt{N} \tag{11.40}$$

In this case, the constellation shown in Figure 5.2 and multiples of it, among others are optimum.

It is interesting to note that for $\phi < 2\pi/3$ the "uniformly spaced" constellation is not optimum. Rather the optimal constellation is that shown in Figure 11.4.

The values of N_1 and $N_2=N_3$ for several values of ϕ are summarized in Table 11.1.

Table 11.1

ϕ	N_1/N	$(N_2/N) = (N_3/N)$
1°	.50	.25
10°	.50	.25
30°	.50	.25
45°	.48	.26
60°	.46	.27
90°	.41	.29
120°	.33	.33

It is clear from the table that the optimum values of N_1/N and $N_2/N = N_3/N$ are almost identical to those in Example 10.1 for $\phi \leq \pi/2$. This is a consequence of the fact that the mean squared error σ^2 is dominated by σ_y^2 over this range of angle.

END OF EXAMPLE

Example 11.4 (Cone Configuration): Consider the problem of placing N beacons within a cone of half angle ϕ so as to minimize total mean squared error σ^2 at the vertex of the cone.

Let C denote a constellation of N beacons confined to the cone. The system of vectors $\underline{i}_1, \underline{i}_2, \ldots \underline{i}_N$ is shown in Figure 11.5. Let the coordinate system (X',Y',Z') be selected as shown.

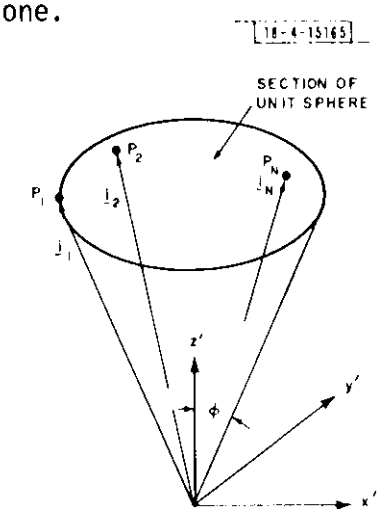

Figure 11.5

An analysis similar to that leading to Equation (11.25) in Example 11.3 shows that

$$\frac{\sigma^2}{(c\sigma_\tau)^2} \geq \frac{1}{N}\left[\frac{1}{1-\overline{(Y')^2}-\overline{Z^2}-(\overline{Z'})^2-(\overline{X'})^2} + \frac{1}{\overline{(Y')^2}-(\overline{Y'})^2} + \frac{1}{\overline{Z^2}}\right]$$

$$\geq \frac{1}{N}\left[\frac{1}{1-\overline{(Y')^2}-\overline{Z^2}-(\overline{Z'})^2} + \frac{1}{\overline{(Y')^2}} + \frac{1}{\overline{Z^2}}\right] \qquad (11.41)$$

with equality holding in (11.41) if and only if $\underline{L}$ = diagonal and $\overline{X'} = \overline{Y'} = 0$.

The results of Appendix II show that $\overline{Z^2}$ satisfies the inequality

$$\overline{Z^2} \leq (1-\overline{Z'})(\overline{Z'}-\cos\phi) \qquad (11.42)$$

with the equal sign applying if and only if the points $P_1, P_2, \ldots P_N$ are confined to the minimum Z' and maximum Z' positions of the spherical

sector as shown in Figure 11.6. It follows from (11.42) that there exists an angle ϕ' satisfying

$$0 \leq \phi' \leq \phi \quad (11.43)$$

such that

$$\overline{Z^2} = (1-\overline{Z}')(\overline{Z}'-\cos\phi') \quad (11.44)$$

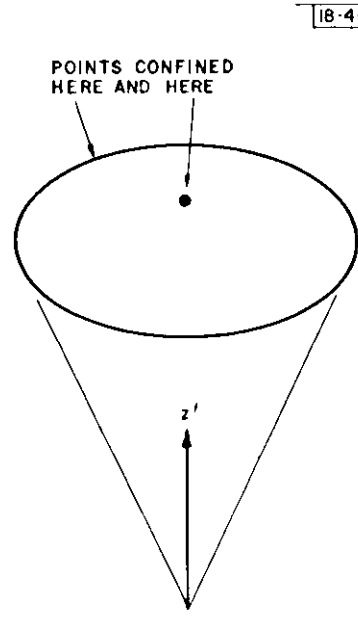

Figure 11.6

Consequently (11.41) can be rewritten

$$\frac{\sigma^2}{(c\sigma_\tau)^2} \geq \frac{1}{N}\left[\frac{1}{1-\overline{(Y')^2}-(1-\overline{Z}')(\overline{Z}'-\cos\phi')-(\overline{Z}')^2} + \frac{1}{\overline{(Y')^2}} + \frac{1}{(1-\overline{Z}')(\overline{Z}'-\cos\phi')}\right]$$

$$= \frac{1}{N}\left[\frac{1}{(1+\cos\phi')(1-\overline{Z}')-\overline{(Y')^2}} + \frac{1}{\overline{(Y')^2}} + \frac{1}{(1-\overline{Z}')(\overline{Z}'-\cos\phi')}\right] \quad (11.45)$$

It follows from (11.45) that

$$\frac{\sigma^2}{(c\sigma_\tau)^2} \geq \frac{1}{N} \underset{\substack{\cos\phi \leq \bar{Z}' \leq 1 \\ \overline{(Y')^2} \leq (1+\cos\phi')(1-\bar{Z}')}}{\text{Minimum}} \left\{ \frac{1}{(1+\cos\phi')(1-\bar{Z}') - \overline{(Y')^2}} + \frac{1}{\overline{(Y')^2}} + \frac{1}{(1-\bar{Z}')(\bar{Z}'-\cos\phi')} \right\} \tag{11.46}$$

$$= \frac{1}{N} \frac{16}{(1+\cos\phi')(\sqrt{1+\cos\phi'} - \sqrt{5-3\cos\phi'})^2} \tag{11.47}$$

$$\geq \frac{1}{N} \underset{0 \leq \phi' \leq \phi}{\text{Minimum}} \left\{ \frac{16}{(1+\cos\phi')(\sqrt{1+\cos\phi'} - \sqrt{5-3\cos\phi'})^2} \right\}$$

$$= \begin{cases} \frac{1}{N} \dfrac{16}{(1+\cos\phi)(\sqrt{1+\cos\phi} - \sqrt{5-3\cos\phi})^2} & \text{for } \phi \leq \cos^{-1}(-\frac{1}{3}) \quad (11.48) \\ \frac{9}{N} & \text{for } \phi > \cos^{-1}(-\frac{1}{3}) \quad (11.49) \end{cases}$$

For $\phi \leq \cos^{-1}(-\frac{1}{3})$ the constellation $C^*(\phi)$ of points shown in Figure 11.7 achieves the bound provided

1. $$N_1 = \frac{N}{4}\left[\frac{\sqrt{(1+\cos\phi)(5-3\cos\phi)} - (1+\cos\phi)}{1-\cos\phi}\right] \tag{11.50}$$

2. $$N_2 = \frac{N}{4}\left[\frac{(5-3\cos\phi) - \sqrt{(1+\cos\phi)(5-3\cos\phi)}}{1-\cos\phi}\right] \tag{11.51}$$

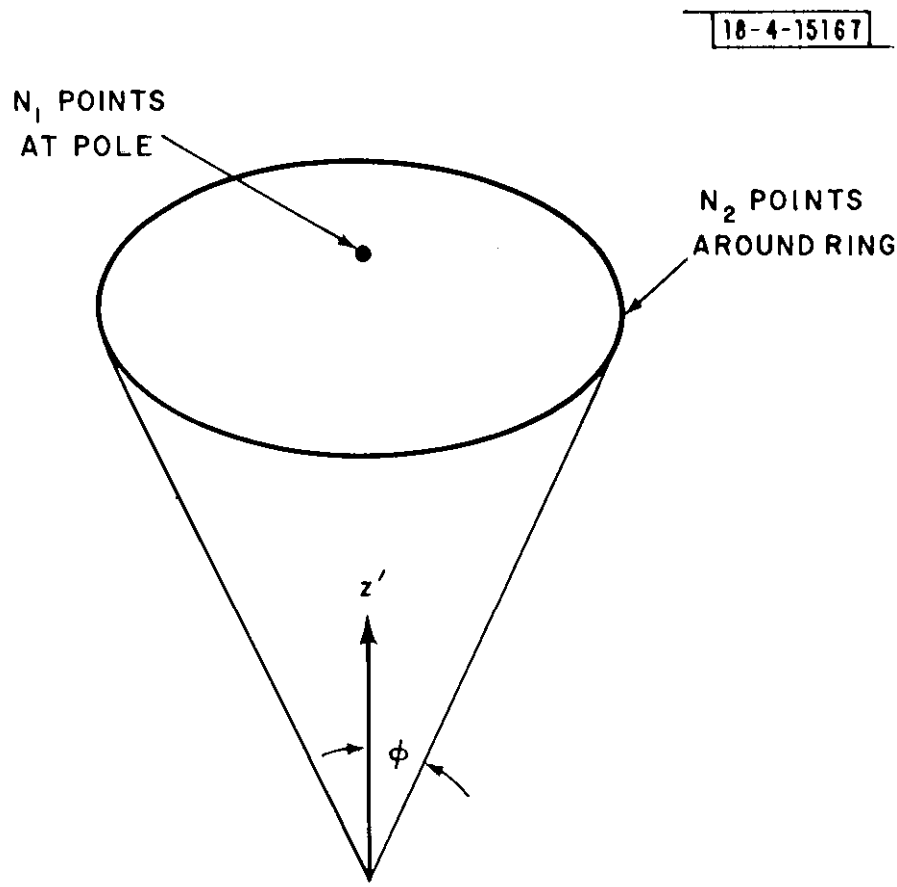

Figure 11.7

3. $\underline{L}$ = diagonal (11.52)

$$\overline{X'} = \overline{Y'} = 0 \tag{11.53}$$

$$\overline{(X')^2} = \overline{(Y')^2} = \frac{\sin^2 \phi}{2} \tag{11.54}$$

The conditions (11.52-11.54) are identical to the optimizing conditions (11.15-11.17) for unrestricted planar arrays, except for the factor $\sin^2 \phi$. Thus (11.52-11.54) assert that the projection of the ring of the N_2 points into the X',Y' plane comprises an optimum two dimensional array, except that the points are distributed along a circle of radius $\sin^4$ rather than the unit circle.

A careful review of the inequalities shows that the constellations satisfying (11.50-11.54) are the only constellations that achieve the bound (11.48).

Thus for $\phi \leq \cos^{-1}(-\frac{1}{3})$ the minimum attainable mean squared error is given by

$$\sigma^2_{min} = (c\sigma_\tau)^2 \frac{1}{N} \frac{16}{(1+\cos\phi)(\sqrt{1+\cos\phi} - \sqrt{3-5\cos\phi})^2} \tag{11.55}$$

The corresponding value of GDOP is

$$GDOP_{min} = \frac{1}{N} \frac{4}{\sqrt{1+\cos\phi}\,(\sqrt{1+\cos\phi} - \sqrt{3-5\cos\phi})^2} \tag{11.56}$$

The minimizing constellation is that shown in Figure 11.7 with (11.50-11.54) being satisfied.

For $\phi \geq \cos^{-1}(-\frac{1}{3})$ any optimum constellation of Example 11.2 that is consistent with the cone restriction achieves the bound (11.49). For example, the optimum N=4 (tetrahedral) constellation achieves the bound (11.49).

Thus for $\phi \geq \cos^{-1}\left(-\frac{1}{3}\right)$ the minimum achievable mean squared error is

$$\sigma^2_{min} = (c\sigma_\tau)^2 \; 9/N \tag{11.57}$$

The corresponding value of GDOP is

$$GDOP_{min} = 3/\sqrt{N} \tag{11.58}$$

The tetrahedral constellation, and multiples of it, among others are optimum.

Representative values of N_1 and N_2 for the optimum constellation are given in Table 11.2.

Table 11.2

ϕ	N_1/N	N_2/N
1°	.500	.500
20°	.485	.515
40°	.447	.553
60°	.395	.605
90°	.309	.691
100°	.279	.721
109.5°	.250	.750

Note as ϕ approaches the "tetrahedral" angle 109.5° ($= \cos^{-1}[-\frac{1}{3}]$) that N_1 and N_2 approach values consistent with the optimum tetrahedral constellation in Figure 11.1 of Example 11.2.

The angular dependence of $GDOP_{min}$ is shown in Figure 11.8. In principle high positional accuracy can be obtained for small values of ϕ by using a sufficient number of satellites. Figure 11.8 shows that the price for

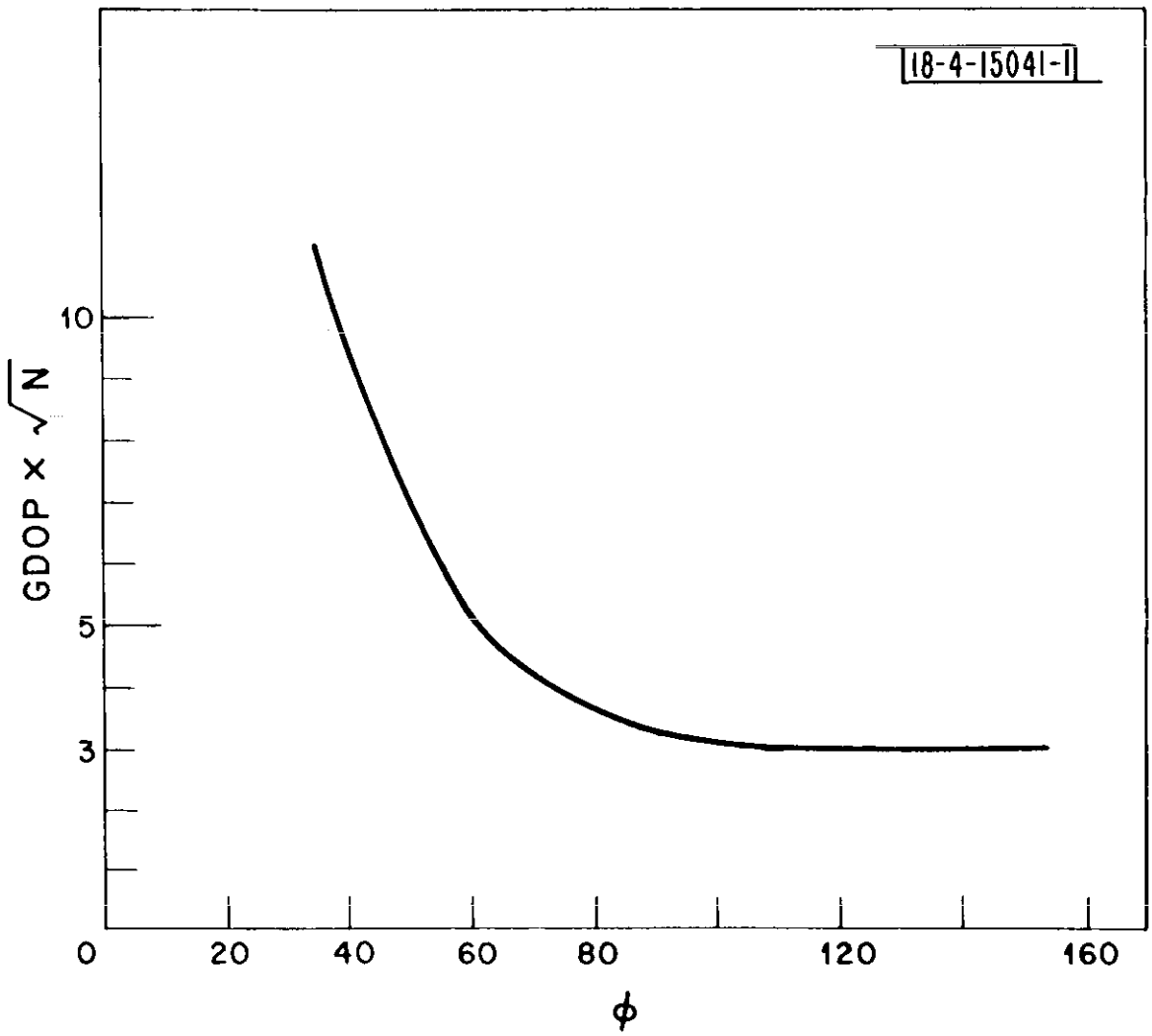

Figure 11.8

such accuracy is high, however.* For example, approximately 24 beacons are required to obtain the same value for GDOP at $\phi = 40°$ as can be obtained with only six beacons at $\phi = 60°$.

Tables 11.3, 11.4 and 11.5 compare the geometric dilutions of several "uniformly spaced" constellations [Example 6.5] with the corresponding values for an optimum constellation for N = 15,100 and infinity. It is clear from the tables that the optimum constellation is modestly better (approx. 10%) in the case of fifteen beacons, is significantly better (approx. 33%) in the case of one hundred beacons, and is substantially better (up to 50%) in the case of larger numbers of beacons.

END OF EXAMPLE

*Also see Section VIII

Table 11.3

GDOP FOR OPTIMUM AND UNIFORM CONSTELLATION
CONTAINING N=15 BEACONS

ϕ	GDOP x $\sqrt{N}$ (optimum)	GDOP x $\sqrt{N}$ (uniform)
20°	34.16	38.17
40°	9.56	10.51
60°	5.05	5.44
90°	3.24	3.44

Table 11.4

GDOP FOR OPTIMUM AND UNIFORM CONSTELLATIONS
CONTAINING N=100 BEACONS

ϕ	GDOP x $\sqrt{N}$ (optimum)	GDOP x $\sqrt{N}$ (uniform)
20°	34.16	48.79
40°	9.56	13.20
60°	5.05	6.62
90°	3.24	3.87

Table 11.5

GDOP FOR OPTIMUM AND UNIFORM CONSTELLATIONS CONTAINING N=∞ BEACONS

ϕ	GDOP x $\sqrt{N}$ (optimum)	GDOP x $\sqrt{N}$ (uniform)
20°	34.16	58.02
40°	9.56	15.42
60°	5.05	7.58
90°	3.24	4.24

XII. SENSITIVITY OF ACCURACY TO SINGLE BEACON DROPOUT

An important consideration in the design of beacon constellations is the sensitivity of system performance to single beacon dropout. In a satellite based surveillance system, dropout can result either from failure of on-board equipment, or from jamming. This section derives relatively simple formulae for calculating the effect on accuracy of such beacon dropout.

Thus let $\underline{L}$ denote the matrix (4.10) for a two dimensional constellation C containing N beacons. Let C_i denote the constellation that results when beacon B_i is removed from C. Assume a coordinate system at the center of mass CM of C that diagonalizes $\underline{L}$.

Removal of beacon B_i from the constellation C changes the $\underline{L}$ matrix in two ways. First the contribution of B_i to the elements of (4.10) must be subtracted out. Second, the center of mass of the constellation changes so that the elements of $\underline{L}$ must be adjusted through use of (6.11)-(6.16). The resultant matrix $\underline{L}_i$ is given by

$$\underline{L}_i = \underline{L} - \underbrace{\begin{bmatrix} X_i \\ Y_i \end{bmatrix} [X_i, Y_i]}_{\text{subtraction of } B_i \text{ terms}} - \underbrace{\frac{1}{N-1} \begin{bmatrix} X_i \\ Y_i \end{bmatrix} [X_i, Y_i]}_{\text{change of CM}} \tag{12.1}$$

$$= \underline{L} - \frac{N}{N-1} \begin{bmatrix} X_i \\ Y_i \end{bmatrix} [X_i, Y_i] \tag{12.2}$$

where X_i and Y_i denote the coordinates of B_i with respect to the center of mass of C.

If σ^2 and σ_i^2 denote respectively the total mean squared errors for the constellations C and C_i, then direct calculation shows that

$$\sigma_i^2 - \sigma^2 = \mathrm{Tr}[\underline{L}_i^{-1}] - \mathrm{Tr}[\underline{L}^{-1}]$$

$$= \frac{\alpha\left[\frac{X_i^2}{L_{xx}^2} + \frac{Y_i^2}{L_{yy}^2}\right]}{1 - \alpha\left[\frac{1}{L_{xx}} X_i^2 + \frac{1}{L_{yy}} Y_i^2\right]} \qquad (12.3)$$

where

$$\alpha = \frac{N}{N-1} \qquad (12.4)$$

Equation (12.3) can be rewritten in terms of an arbitrary coordinate system (X',Y') centered at CM as follows

$$\sigma_i^2 - \sigma^2 = \frac{\alpha \underline{X}_t (\underline{L}')^2 \underline{X}}{1 - \alpha \underline{X}_t (\underline{L}')^{-1} \underline{X}} \qquad (12.5)$$

Here $\underline{L}'$ denotes the matrix (4.10) calculated in terms of X',Y' and $\underline{X}$ denotes a 2 x 1 vector the elements of which are the coordinates of B_i in the system (X',Y').

An analogous derivation shows that for three dimensional systems

$$\sigma_i^2 - \sigma^2 = \frac{\alpha\left[\frac{X_i^2}{L_{xx}^2} + \frac{Y_i^2}{L_{yy}^2} + \frac{Z_i^2}{L_{zz}^2}\right]}{1 - \alpha\left[\frac{X_i^2}{L_{xx}} + \frac{Y_i^2}{L_{yy}} + \frac{Z_i^2}{L_{zz}}\right]} \qquad (12.6)$$

where once again the coordinate system at CM is selected to diagonalize $\underline{L}$. Equation (12.5) is directly applicable to three dimensions provided $\underline{X}$ and $\underline{L}'$ are interpreted in the obvious manner.

One expects the total mean squared error to increase when a beacon drops out. Equations (12.3) and (12.6) show that this is the case. The denominators in both equations are positive since both represent the quotient of determinants $|\underline{L}_i|/|\underline{L}|$, and the matrices $\underline{L}_i$ and $\underline{L}$ are positive definite. Consequently

$$\sigma_i^2 - \sigma^2 > 0 \tag{12.7}$$

The following example illustrates use of Equation (12.6).

Example 12.1 Consider the uniform distribution of beacons shown in Figure 5.6. Assume it is desired to assess the effect of dropout of the polar beacon (i.e. point P_1).

One method of calculating the change in total mean squared error due to dropout is to calculate the mean squared error σ^2 for the constellation of Figure 5.6, and that (σ_1^2) for the constellation minus point P_1, and then take the difference. This method shows that

$$\sigma^2 = .827 \tag{12.8}$$

$$\sigma_1^2 = .949 \tag{12.9}$$

$$\sigma_1^2 - \sigma^2 = .949 - .827 = .122 \tag{12.10}$$

Equation (12.6) provides an alternate and faster method for calculating the change $\sigma_1^2 - \sigma^2$. Specifically (12.6) shows that

$$\sigma_1^2 - \sigma^2 = \frac{\alpha \dfrac{Z_1^2}{(L_{zz})^2}}{1 - \alpha \dfrac{Z_1^2}{L_{zz}}} = \frac{\left(\frac{15}{14}\right)\left(\frac{.65}{2.16}\right)^2}{1 - \left(\frac{15}{14}\right)\frac{(.65)^2}{2.16}} \tag{12.11}$$

$$= .122$$

END OF EXAMPLE

Often it is desirable to know which beacon dropout will most impact the total mean squared error σ^2. Equation (12.6) provides a simple answer to this question for the important case of a cone restricted beacon constellation where

$$L_{zz} << L_{xx} \quad \text{and} \quad L_{zz} << L_{yy} \tag{12.12,13}$$

(see Section IX). Here (12.6) reduces to

$$\sigma_i^2 - \sigma^2 \approx \frac{1}{L_{zz}} \left[\frac{\alpha \frac{Z_i^2}{L_{zz}}}{1 - \alpha \frac{Z_i^2}{L_{zz}}} \right] \tag{12.14}$$

with

$$\alpha \frac{z_i^2}{L_{zz}} < 1 \tag{12.15}$$

Clearly the change (12.14) is maximized by the point P_i having the maximum value of Z_i; that is, by the point P_i most removed in the Z direction from the center of mass. Thus for a reasonably uniform cone restricted beacon constellation, accuracy is most impacted by dropout of a satellite either directly overhead, or near the horizon. Clearly if most of the beacons are directly overhead, then accuracy is most impaired by dropout of a beacon on the cone horizon. On the other hand if most of the beacons are near the cone horizon, then accuracy is most impaired by dropout of a beacon overhead.*

The conclusion that accuracy is most sensitive to overhead and horizon beacons complements the results on optimal beacon constellations obtained in

---

*The objective here is to make the resulting set of beacon images as nearly planar as possible. See Example 5.3.

Examples 10.2 and 11.4. In effect the examples show that accuracy is most improved by placing beacons directly overhead and on the horizon. Thus it is quite reasonable that accuracy should be most impaired by removing beacons from these same positions.

XIII. GROUND BASED MULTILATERATION SYSTEMS

In ground based hyperbolic multilateration systems the beacons tend to lie in a plane; moreover the spacing between the beacons greatly exceeds the altitude of the subject (aircraft) above the plane. These facts limit the accuracy with which ground based systems can determine altitude.

The following examples utilize the results of Section IV to obtain useful bounds on the ability of ground based systems to measure altitude.

Example 13.1 Assume that no beacons are in the immediate vicinity of the aircraft so that the (N) beacon images lie within a band of the unit sphere as shown in Fig. 13.1. Let the coordinate system (X,Y,Z) be selected so that the Z axis coincides with the vertical as shown.

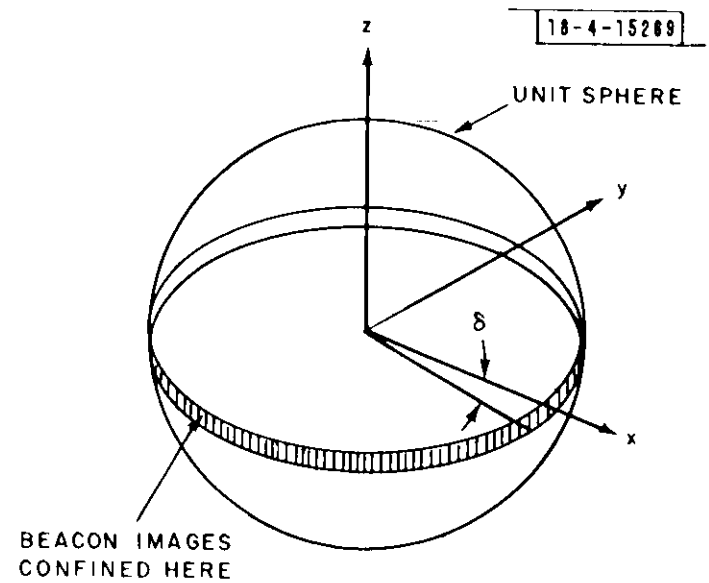

Figure 13.1

Clearly the Z-directed moment arms are strongly disadvantaged. Thus L_{zz} is small, and the error magnification factor Γ_{zz} is corresponding large. This observation can be quantified as follows.

By reasoning as in Appendix II it is easy to show that $\overline{Z^2}$ is bounded as follows

$$\overline{Z^2} \leq -\overline{Z}\,(\sin\delta + \overline{Z}) \tag{13.1}$$

so that

$$\overline{Z^2} \leq \underset{0 \leq \overline{Z} \leq -\sin\delta}{\text{Maximum}} \; -\overline{Z}(\overline{Z} + \sin\delta)$$

$$= \frac{\sin^2\delta}{4} \tag{13.2}$$

Therefore

$$L_{zz} = N\,\overline{Z^2}$$

$$\leq N\,\frac{\sin^2\delta}{4} \tag{13.3}$$

It follows from Eq. (A1.3) of Appendix I that

$$\Gamma_{zz} \geq \frac{1}{L_{zz}}$$

$$\geq \frac{4}{N\sin^2\delta} \tag{13.4}$$

Consequently the RMS altitude error (σ_z) and the RMS ranging error ($c\sigma_t$) satisfy

$$\frac{\sigma_z}{(c\sigma_t)} = (\Gamma_{zz})^{1/2} = \frac{2}{\sqrt{N}\sin\delta} \tag{13.5}$$

Thus for example with N=4 beacons and $\delta = 10°$ the RMS altitude error exceeds the RMS ranging error by a factor of more than 5.75.

END OF EXAMPLE

Example 13.2* Assume that one beacon B_1 is in the vicinity of the aircraft, but that all other beacons $B_2..B_N$ are far removed from the aircraft. In this case the images $P_1..P_N$ of the beacons on the unit sphere are as shown in Figure 13.2. Let the coordinate system (X,Y,Z) be selected as shown.

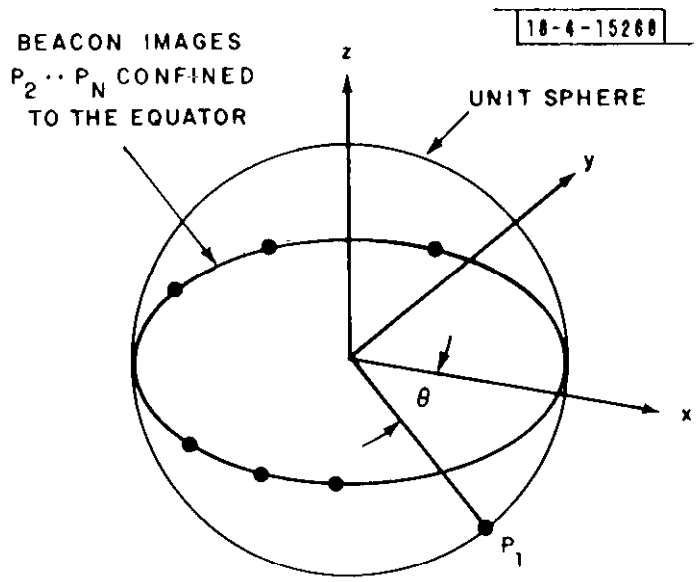

Figure 13.2

The Z coordinate of the center of mass is given by

$$\bar{Z} = -\frac{1}{N} \sin \theta \tag{13.6}$$

consequently

$$L_{zz} = (N-1)\left[-\frac{1}{N} \sin\theta\right]^2 + (1)\left[\left(1 - \frac{1}{N}\right) \sin\theta\right]^2$$

$$= \frac{N-1}{N} \sin^2\theta$$

$$< \sin^2\theta \tag{13.7}$$

It follows that

$$r_{zz} \geq \frac{1}{L_{zz}} > \frac{1}{\sin^2\theta} \tag{13.8}$$

*Result suggested by J. Evans

so that the RMS altitude and ranging errors satisfy

$$\frac{\sigma_z}{(c\sigma_t)} > \frac{1}{\sin\theta}$$

$$= \frac{\text{distance from aircraft to } B_1}{\text{altitude}} \qquad (13.9)$$

Inequality (13.9) shows that only the beacon B_1 nearest to the aircraft is effective in providing altitude discrimination. Moreover the effectiveness of B_1 decreases rapidly as the beacon to aircraft distance exceeds the aircraft altitude.

END OF EXAMPLE

XIV. THE EFFECT ON ACCURACY OF CORRELATED NOISE

The estimate of position (3.7) is a useful one when the TOA errors can be assumed to be uncorrelated and of equal variance. Often, however, the errors have different variances and may be correlated. In such cases the estimate (3.7) may not be the best one.

It is a relatively straightforward task to modify the derivation of (3.7) to take account of TOA errors that are correlated and have unequal variances. The key is to select the estimate of position to be that position which minimizes the quadratic form

$$Q = \underline{\varepsilon}' \underline{P}_{\varepsilon}^{-1} \underline{\varepsilon} \tag{14.1}$$

rather than that which minimizes $\underline{\varepsilon}' \underline{\varepsilon}$, where $\underline{P}_{\varepsilon}$ denotes the correlation matrix for the noise vector $\underline{\varepsilon}$ (see Section III). In the case of Gaussian noise, this decision amounts to a maximum likelihood estimate of position. The resulting estimate is given by

$$\begin{aligned} \underline{\Delta R}^{*} = {} & c[\underline{F}'\underline{H}'(\underline{H}\,\underline{P}_{\varepsilon}\,\underline{H}')^{-1}\,\underline{H}\,\underline{F}]^{-1}\,\underline{F}'\underline{H}'\,(\underline{H}\,\underline{P}_{\varepsilon}\,\underline{H}')^{-1}\,\underline{\Delta T} \\ & -[\underline{F}'\underline{H}'(\underline{H}\,\underline{P}_{\varepsilon}\,\underline{H}')^{-1}\,\underline{H}\,\underline{F}]^{-1}\,\underline{F}'\underline{H}'\,(\underline{H}\,\underline{P}_{\varepsilon}\,\underline{H}')^{-1}\,\underline{H}\,\underline{R} \end{aligned} \tag{14.2}$$

where c, $\underline{R}$, $\underline{\Delta T}$, $\underline{F}$ and $\underline{H}$ are as in Section III.

The estimate of position (14.2) shares an important attribute with the previous estimate (3.7); namely both estimates are insensitive to a common additive noise term ε_0 in the noise sources ε_i. This conclusion follows most directly from an examination of Eq. (3.3). Clearly pairs of ε_0 terms cancel in the left hand members and consequently do not influence the estimate of position. The same conclusion can be drawn from (14.2) by noting that a common noise term has the effect of adding an increment of the form

$$\underline{P}_o = \sigma_o^2 \begin{bmatrix} 1 & 1 & .. & 1 \\ 1 & 1 & .. & 1 \\ . & . & & . \\ . & . & & . \\ 1 & 1 & .. & 1 \end{bmatrix} \tag{14.3}$$

to the correlation matrix $\underline{P}_\varepsilon$. But

$$\underline{H} \begin{bmatrix} 1 & 1 & .. & 1 \\ 1 & 1 & .. & 1 \\ . & . & & . \\ . & . & & . \\ 1 & 1 & .. & 1 \end{bmatrix} \underline{H}' = 0 \tag{14.4}$$

so that $\underline{P}_o$ does not impact the estimate (14.2).

Use of the estimate (14.2) in a satellite surveillance system would require that the matrix $\underline{P}_\varepsilon$ be updated periodically to reflect changes in orbital uncertainties, changes in atmospheric conditions etc. Consequently, apart from ocasionally updating $\underline{P}_\varepsilon$, the computational effort required to calculate the estimate (14.2) is identical with that required for the previous estimate (3.7).

An attractive feature of (14.2) is that it provides a way of taking account of the power levels of received signals when estimating position. This is desirable to minimize the effects of scintillation and/or channel fading. The basic idea is to use the power levels of the received pulses to formulate the correlation matrix $\underline{P}_\varepsilon$ to be used in (14.2) Specifically the correlation matrix $\underline{P}_\varepsilon$ can be separated into two parts as follows

$$\underline{P}_\varepsilon = \underline{P}_{\varepsilon r} + \underline{P}_{\varepsilon o} \tag{14.5}$$

where

$\underline{P}_{\varepsilon r}$ = a diagonal matrix the elements of which are the mean squared time of arrival (TOA) errors that result in the receiver from detecting a signal embedded in noise.

$\underline{P}_{\varepsilon o}$ = a correlation matrix taking account of TOA errors external to the receiver.

The elements of $\underline{P}_{\varepsilon r}$ are a (known) function of the signal to noise ratio in the receiver, and the detection algorithm used. Thus $\underline{P}_{\varepsilon r}$ can be recomputed every time the power level of one of the received signals changes significantly. $\underline{P}_{\varepsilon o}$ need be updated only when conditions external to the receiver change. The resultant correlation matrix (14.5) then can be used in the estimate of position (14.2)

The positional error covariance matrix for the estimate (14.2) is given by

$$\underline{P}_r = c^2 \left[\underline{F}' \underline{H}' (\underline{H} \underline{P}_{\varepsilon} \underline{H}')^{-1} \underline{H} \underline{F}\right]^{-1} \tag{14.6}$$

$$= (c\sigma_o)^2 \underline{\Gamma} \tag{14.7}$$

where C is the velocity of light, and σ_o^2 is a reference variance.

In the case of uncorrelated noise sources with unequal variance, the interpretation of the matrix $\underline{\Gamma}^{-1}$ given in Section IV applies with only one change; namely masses of value (σ_o^2/σ_i^2) rather than unit masses are placed at the points P_i. The entries in $\underline{\Gamma}^{-1}$ then are the various second moments of the mass constellation about its center of mass. That is,

$$\underline{L} = \underline{\Gamma}^{-1} = \begin{bmatrix} \sum_{i=1}^{N} \frac{\sigma_o^2}{\sigma_i^2} X_i^2 & \sum_{i=1}^{N} \frac{\sigma_o^2}{\sigma_i^2} X_i Y_i & \sum_{i=1}^{N} \frac{\sigma_o^2}{\sigma_i^2} X_i Z_i \\ \sum_{i=1}^{N} \frac{\sigma_o^2}{\sigma_i^2} X_i Y_i & \sum_{i=1}^{N} \frac{\sigma_o^2}{\sigma_i^2} Y_i^2 & \sum_{i=1}^{N} \frac{\sigma_o^2}{\sigma_i^2} Y_i Z_i \\ \sum_{i=1}^{N} \frac{\sigma_o^2}{\sigma_i^2} X_i Z_i & \sum_{i=1}^{N} \frac{\sigma_o^2}{\sigma_i^2} Y_i Z_i & \sum_{i=1}^{N} \frac{\sigma_i^2}{\sigma_i^2} Z_i^2 \end{bmatrix} \tag{14.8}$$

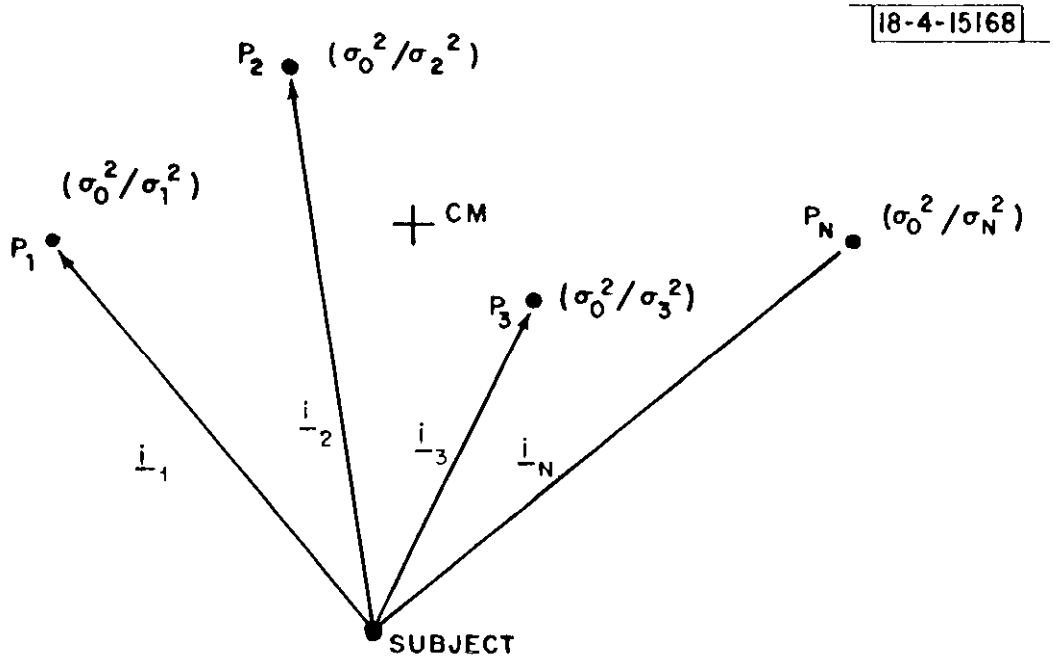
18-4-15168
P2
(σ0²/σ2²)
(σ0²/σ1²)
CM
P1
PN
(σ0²/σN²)
P3
(σ0²/σ3²)
i2
i3
i1
iN
SUBJECT

Figure 14.1

where X_i, Y_i, and Z_i are the coordinates of the points P_i with respect to the center of mass as shown in Figure 14.1. The derivation of (14.8) parallels that of (4.7) and, accordingly, is omitted.

The results of Sections V-XII apply with only minor modifications to the case of uncorrelated noise sources with unequal variances. The primary modifications are noted below

Section	Changes
Section V (calculation of $\underline{\Gamma}$)	Replace unit masses by masses of value σ_o^2/σ_i^2.
Section VI (Approximations)	The notion of approximating discrete averages by continuous averages still applies. A weighting factor must be introduced into the integrals to account for unequal masses.
Sections VII-IX (Accuracy Dependence)	No changes.
Sections X,XI (Error Minimization)	The results hold with only one change; namely the fractions representing the proportions of the total number of beacons to be placed in key locations now represent the proportions of the total <u>mass</u> to be placed in the same locations.
Section XII (Sensitivity)	Use the following value for α in place of N/N-1

$$\alpha = \frac{\sigma_o^2}{\sigma_i^2} \frac{\sum_{i=1}^{N} \frac{\sigma_o^2}{\sigma_i^2}}{\left(\sum_{i=1}^{N} \frac{\sigma_o^2}{\sigma_i^2}\right) - \frac{\sigma_o^2}{\sigma_i^2}}$$

XV. INDEPENDENT ALTITUDE MEASUREMENT

The results of Sections IX and XIII show that altitude errors typically exceed horizontal errors for cone restricted or ground based beacon constellations. One method for improving altitude accuracy is to utilize an independent measurement of altitude. For example an independent altitude measurement can be obtained from a barometric altimeter. The present section shows how the results of Sections III, IV and XIV can be extended to accommodate such a measurement.

Thus let (X',Y',Z') denote a three dimensional coordinate system selected so that measurement along the Z' axis corresponds to altitude. The independent altitude measurement can be represented by the equation

$$Z' - \epsilon_z = Z'_r + [0,0,-1] \cdot \underline{\Delta R} \qquad (15.1)$$

where

Z' = the actual altitude

ϵ_z = the error made in measuring Z'

$Z' - \epsilon_z$ = the measured altitude

Z'_r = the Z' coordinate of the reference point (see Figure 3.2)

$\underline{\Delta R}$ = a vector specifying subject location with respect to the reference point (see Figure 3.2)

The equations for the measured quantities now are given by Equations (3.3) and (15.1). These equations are collected below for convenient reference, with Equation (15.1) divided by c.

$$
\begin{aligned}
(\tau_1 - \tau_2) + (\varepsilon_1 - \varepsilon_2) &= (r_1 - r_2)/c + (\underline{i}_1 - \underline{i}_2) \cdot \Delta\underline{R}/c \\
&\vdots \\
(\tau_{N-1} - \tau_N) + (\varepsilon_{N-1} - \varepsilon_N) &= (r_{N-1} - r_N)/c + (\underline{i}_{N-1} - \underline{i}_N) \cdot \Delta\underline{R}/c \\
Z'/c - \varepsilon_z/c &= Z_r/c + [0,0,-1] \cdot \Delta\underline{R}/c
\end{aligned}
\tag{15.2}
$$

Equations (15.2) can be re-written as the single matrix equation

$$
\underline{\Delta T} - \underline{H}\,\underline{\varepsilon} = \frac{1}{c}\,\underline{H}\,\underline{R} + \frac{1}{c}\,\underline{H}\,\underline{F}\,\underline{\Delta R} \tag{15.3}
$$

with the understandings that

$\underline{\Delta T}$ = an N element vector the first N-1 elements of which equal the TOA differences $\tau_j - \tau_{j+1}$, and the Nth element of which equals Z'/c. (15.4)

$\underline{\varepsilon}$ = an N+1 element vector the first N elements of which equal ε_j $(1 \le j \le N)$, and the (N+1)th element of which equals ε_z/c (15.5)

$\underline{R}$ = an N+1 element vector the first N elements of which are the $r_j (1 \le j \le N)$, and the (N+1)th element of which equals Z_r (15.6)

$\underline{F}$ = an (N+1)x 3 matrix the first N rows of which each contain the three components of the unit vector $\underline{i}_j$ pointing to the jth beacon, and the (N+1)th row of which consists of the vector [0,0,-1]. (15.7)

$\underline{H}$ = an Nx(N+1) matrix of the form

$$\underline{H} = \begin{bmatrix} 1 & -1 & 0 & \cdots & 0 & 0 \\ 0 & 1 & -1 & & 0 & 0 \\ \vdots & \vdots & \vdots & & \vdots & \vdots \\ 0 & 0 & 0 & 0 \quad 1 & -1 & 0 \\ 0 & 0 & 0 & 0 \quad 0 & 0 & 1 \end{bmatrix} \left.\vphantom{\begin{bmatrix} 1 \\ 1 \\ \vdots \\ 1 \\ 1 \end{bmatrix}}\right\} N \text{ rows}$$

$$\underbrace{\qquad\qquad\qquad\qquad\qquad\qquad}_{N+1 \text{ columns}} \tag{15.8}$$

The least squares estimate of subject position can be found from (15.3) exactly as in Section XIV. Equation (14.2) continues to express the result with $\underline{\Delta T}$, $\underline{R}$, $\underline{F}$ and $\underline{H}$ given by (15.4)-(15.8) and

$$\underline{P}_{\underline{\varepsilon}} = \text{Expected Value of } [\underline{\varepsilon}\ \underline{\varepsilon}'] \tag{15.9}$$

with $\underline{\varepsilon}$ given by (15.5).

The covariance matrix for the positional error continues to be given by (14.6), (14.7).

In the case where all measurement errors are uncorrelated it can be shown that the inverse of the error magnification matrix $\underline{r}$ in (14.7) is given by

$$\underline{r}^{-1} = \begin{bmatrix} L_{xx} & L_{xy} & L_{xz} \\ L_{xy} & L_{yy} & L_{yz} \\ L_{xz} & L_{yz} & L_{zz} \end{bmatrix} + \begin{bmatrix} 0 & 0 & 0 \\ 0 & 0 & 0 \\ 0 & 0 & (\sigma_o c)^2/\sigma_z^2 \end{bmatrix} \tag{15.10}$$

where $L_{\alpha\beta}$ denotes the α-β entry in the matrix (14.8) and σ_z^2 denotes the expected value of $(\varepsilon_z)^2$. That is, $\underline{r}^{-1}$ is computed exactly as in Section XIV

except that the quantity $(\sigma_o c)^2/\sigma_z^2$ now must be added to the Z-Z element of $\underline{\Gamma}^{-1}$. Thus the effect of the independent altitude measurement is to increase the Z-Z element of $\underline{\Gamma}^{-1}$ and correspondingly to reduce Γ_{zz}.

The effect of a highly accurate altitude measurement can be assessed by examining the limiting form of $\underline{\Gamma}$ as $\sigma_z \to 0$. It is clear from (15.10) that

$$\lim_{\sigma_z \to 0} \underline{\Gamma} = \begin{bmatrix} \begin{bmatrix} L_{xx} & L_{xy} \\ L_{xy} & L_{yy} \end{bmatrix}^{-1} & \begin{matrix} 0 \\ 0 \end{matrix} \\ \begin{matrix} 0 & 0 \end{matrix} & 0 \end{bmatrix} \tag{15.11}$$

Thus the error magnification factors Γ_{xx} and Γ_{yy} can be found from the expressions

$$\Gamma_{xx} = \frac{L_{yy}}{L_{xx}L_{yy} - (L_{xy})^2} \tag{15.12}$$

$$\Gamma_{yy} = \frac{L_{xx}}{L_{xx}L_{yy} - (L_{xy})^2} \tag{15.13}$$

where L_{xx}, L_{xy} and L_{yy} are calculated by the method of Section XIV or IV. For small but non-vanishing σ_z it can be shown that the error magnification factor Γ_{zz} is given by

$$\Gamma_{xx} \approx \sigma_z^2/(\sigma_o c)^2 \tag{15.14}$$

as expected.

REFERENCES

1. N. Marchand, "Error Distributions of Best Estimate of Position from Multiple Time Differance Hyperbolic Networks", IEEE Transactions on Aerospace and Navigational Electronics, pp. 96-100; June 1964.

2. D. L. Snyder, "Navigation with High Altitude Satellites: A Study of Errors in Position Determination", MIT Lincoln Laboratory Technical Note 1967-11.

3. C. D. Sullivan, "Navigation with High Altitude Satellites: A Study of the Effects of Satellite-User Geometry on Position Accuracy" MIT Lincoln Laboratory Technical Note 1967-18.

4. T. J. Goblick and D. L. Snyder "Analysis of Position Fix Accuracy Using High Altitude Satellites", private communication.

5. I. G. Stiglitz,et. al. "Concept Formulation Studies of the Surveillance Aspects of the Fourth Generation Air Traffic Control System", MIT Lincoln Laboratory Project Report ATC-7; September 1971.

6. D. C. Cooper, "Statistical Analysis of Position-Fixing; General Theory for Systems with Gaussian Errors", Proc. I.E.E. Vol. 119, No. 6, June 1972.

7. N. E. Nahi, "Estimation Theory and It's Applications", Wiley 1969.

8. E. J. Kelly, "The Use of Supplementary Receivers for Enhanced Positional Accuracy in the DAB System", MIT Lincoln Laboratory Technical Note 1972-38; December 1972.

APPENDIX I

The inequalities required in Sections VII, X and XI are direct consequences of the following theorem.

Theorem: Let

$$\underline{\Gamma} = \begin{bmatrix} \Gamma_{11} & \Gamma_{12} \cdots \Gamma_{1N} \\ \Gamma_{12} & \Gamma_{22} \cdots \Gamma_{2N} \\ \vdots & \\ \Gamma_{1N} & \Gamma_{2N} \cdots \Gamma_{NN} \end{bmatrix} \tag{A1.1}$$

be a symmetric positive definite matrix. Let

$$\underline{L} = \begin{bmatrix} L_{11} & L_{12} \cdots L_{1N} \\ L_{12} & L_{22} \cdots L_{2N} \\ \vdots & \vdots \quad \vdots \\ L_{1N} & L_{2N} \quad L_{NN} \end{bmatrix} \tag{A1.2}$$

denote the inverse of $\underline{\Gamma}$. Then

$$\Gamma_{ii} \geq \frac{1}{L_{ii}} \qquad i = 1,2,..N \tag{A1.3}$$

Moreover equality holds if and only if

$$\Gamma_{ij} = 0 \qquad \text{for } j \neq i \tag{A1.4}$$

or equivalently

$$L_{ij} = 0 \qquad \text{for } j \neq i \quad . \tag{A1.5}$$

Proof: The proof starts from the identity

$$L_{ii} = [L_{i1}, L_{i2}, \ldots L_{iN}] \begin{bmatrix} \Gamma_{11} & \Gamma_{12} & \cdots & \Gamma_{1N} \\ \Gamma_{12} & \Gamma_{22} & \cdots & \Gamma_{2N} \\ \vdots & \vdots & & \vdots \\ \Gamma_{1N} & \Gamma_{2N} & \cdots & \Gamma_{NN} \end{bmatrix} \begin{bmatrix} L_{i1} \\ L_{i2} \\ \vdots \\ L_{iN} \end{bmatrix} \tag{A1.6}$$

Decompose the column vector $[L_{i1}, L_{i2}, \ldots L_{iN}]'$ into two vectors $\underline{L}_d$ and $\underline{L}_o$ where $\underline{L}_d$ is null except for the ith entry which is L_{ii}, and $\underline{L}_o$ which is identical to $[\underline{L}_{i1}, L_{i2}, \ldots L_{iN}]'$ except that L_{ii} is replaced by zero. Equation (A1.6) then takes the form

$$\begin{aligned} L_{ii} &= (\underline{L}_d + L_o)' \ \underline{\Gamma} \ (\underline{L}_d + \underline{L}_o) \\ &= 2 \ \underline{L}'_d \ \underline{\Gamma} \ (\underline{L}_d + \underline{L}_o) - \underline{L}'_d \ \underline{\Gamma} \ \underline{L}_d + \underline{L}'_o \ \underline{\Gamma} \ \underline{L}_o \end{aligned} \tag{A1.7}$$

Direction calculation shows that

$$\underline{L}'_d \ \underline{\Gamma} \ (\underline{L}_d + \underline{L}_o) = L_{ii} \tag{A1.8}$$

$$\underline{L}'_d \ \underline{\Gamma} \ \underline{L}_d = \Gamma_{ii}(L_{ii})^2 \tag{A1.9}$$

Use of (A1.8) and (A1.9) in (A1.7) shows that

$$\Gamma_{ii} = \frac{1}{L_{ii}} + \frac{1}{(L_{ii})^2} \ \underline{L}'_o \ \underline{\Gamma} \ \underline{L}_o \tag{A1.10}$$

$$\geq \frac{1}{L_{ii}} \tag{A1.11}$$

The second term in (A1.10) equals zero if and only if $\underline{L}_o = 0$ since $\underline{\Gamma}$ is assumed positive definite. Consequently equality in (A1.3) holds if and only if (A1.5) is satisfied.

Q.E.D.

APPENDIX II

Proof* That $\overline{Y^2} \leq (1-\overline{Y'})(\overline{Y'} - \cos\phi)$

The quantity of interest

$$\overline{Y^2} = \frac{1}{N} \sum_{i=1}^{N} (Y_i-\overline{Y})^2 \tag{A2.1}$$

can be interpreted as the sum of the ordinates of the points shown in Figure A2.1. The line L given by

$$\begin{aligned} Z &= (\overline{Y}-\cos\phi)^2 + \frac{(\overline{Y}-1)^2 - (\overline{Y}-\cos\phi)^2}{1-\cos\phi} (y-\cos\phi) \\ &= (\overline{Y}-\cos\phi)^2 + (1+\cos\phi-2\overline{Y})(y-\cos\phi) \end{aligned} \tag{A2.2}$$

connects the points $(\cos\phi, [\cos\phi - \overline{Y'}]^2)$ and $(1, [1-\overline{Y'}]^2)$. Clearly L overbounds the parabola $z = (y-\overline{Y'})^2$ on the interval $\cos\phi \leq y \leq 1$. That is,

$$(Y_i-\overline{Y})^2 \leq (\overline{Y}-\cos\phi)^2 + (1+\cos\phi-2\overline{Y})(Y_i-\cos\phi) \tag{A2.3}$$

for $\cos\phi \leq Y_i \leq 1$, with the equal sign applying only if

$$Y_i = \cos\phi \quad \text{or} \quad Y_i = 1 \tag{A2.4}$$

Consequently

$$\overline{Y^2} = \frac{1}{N} \sum_{i=1}^{N} (Y_i-\overline{Y})^2 \leq \frac{1}{N} \sum_{i=1}^{N} (\overline{Y}-\cos\phi)^2 + (1+\cos\phi-2\overline{Y})(Y_i-\cos\phi)$$

$$= (1-\overline{Y'})(\overline{Y'}-\cos\phi)$$

with equality holding if and only if (A2.4) is satisfied for $i = 1,2,\ldots N$.

*Proof suggested by I. G. Stiglitz

18-4-15169

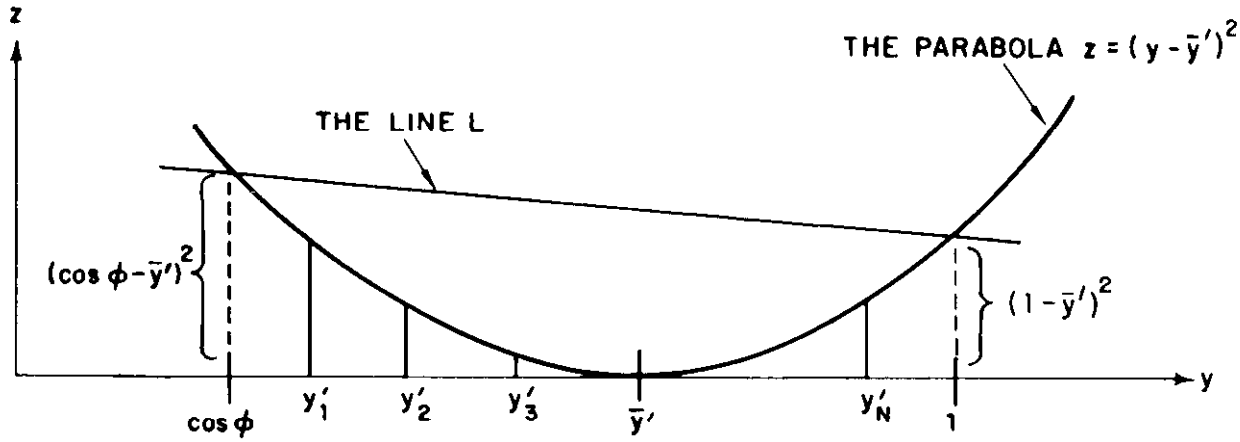

Figure A2.1

APPENDIX III

Proof of Inequality (9.4)

Let C be a constellation of N beacons confined to the sector shown in Figure 9.1. Assume C is such that the center of mass of $P_1, P_2, \ldots P_N$ lies on the sector centerline. That is, assume $\overline{X'} = 0$.

The reasoning leading to (11.6), (11.7) shows that

$$L_{xx} = N\,[1-\overline{(Y')^2}] = N\,[1 - \overline{Y^2} - (\overline{Y'})^2] \tag{A3.1}$$

$$L_{yy} = N\,\overline{Y^2} \tag{A3.2}$$

where $\overline{(Y')^2}$, $\overline{Y^2}$ and $\overline{Y'}$ are as in Section XI. Thus the ratio of interest is given by

$$\frac{L_{xx}}{L_{yy}} = \frac{1 - \overline{Y^2} - (\overline{Y'})^2}{\overline{Y^2}} = \frac{1 - (\overline{Y'})^2}{\overline{Y^2}} - 1 \tag{A3.3}$$

Use of inequality (A2.5) in (A3.3) shows that

$$\frac{L_{xx}}{L_{yy}} \geq \frac{1 + \overline{Y'}}{\overline{Y'} - \cos\phi} - 1 \tag{A3.4}$$

Clearly

$$\frac{L_{xx}}{L_{yy}} \geq \underset{\cos\phi \leq \overline{Y'} \leq 1}{\text{Minimum}} \left\{ \frac{1+\overline{Y'}}{\overline{Y'}-\cos\phi} - 1 \right\}$$

$$= \operatorname{Tan}^2\left(\frac{\pi}{2} - \frac{\phi}{2}\right) \tag{A3.5}$$

Q.E.D.

Proof of Inequality (9.7)

Let C be a constellation of N beacons confined to the cone shown in Figure 10.4. Assume C is such that the center of mass CM of points $P_1, P_2, \ldots P_N$ lies on the cone axis. That is assume, $\overline{X}' = \overline{Y}' = 0$. Assume further that the coordinate system X,Y,Z is set up at CM so that the Z axis coincides with the cone axis, and so that

$$L_{xy} = 0 \tag{A3.6}$$

The ratios σ_z^2/σ_x^2 and σ_z^2/σ_y^2 satisfy the conditions

$$\frac{\sigma_z^2}{\sigma_x^2} = \frac{\Gamma_{zz}}{\Gamma_{xx}} = \frac{L_{xx}\, L_{yy}}{L_{yy}\, L_{zz} - L_{yz}^2} \geq \frac{L_{xx}}{L_{zz}} \tag{A3.7}$$

$$\frac{\sigma_z^2}{\sigma_y^2} = \frac{\Gamma_{zz}}{\Gamma_{yy}} = \frac{L_{xx}\, L_{yy}}{L_{xx}\, L_{zz} - L_{xz}^2} \geq \frac{L_{yy}}{L_{zz}} \tag{A3.8}$$

Addition of (A3.7) and (A3.8) shows that the quantity of interest satisfies

$$\frac{\sigma_z^2}{\sigma_x^2} + \frac{\sigma_z^2}{\sigma_y^2} \geq \frac{L_{xx} + L_{yy}}{L_{zz}} \tag{A3.9}$$

The reasoning leading to Equations (11.6) and (11.7) shows that

$$L_{xx} = N\,[1 - \overline{Y^2} - \overline{Z^2} - (\overline{Z'})^2] \tag{A3.10}$$

$$L_{yy} = N\,\overline{Y^2} \tag{A3.11}$$

$$L_{zz} = N\,\overline{Z^2} \tag{A3.12}$$

where $\overline{Y^2}$, $\overline{Z^2}$ and $\overline{Z'}$ are as in Section XI. Use of (A3.10), (A3.11) and (A3.12) in (A2.9) produces an expression analagous to (A3.3); namely

$$\frac{\sigma_z^2}{\sigma_x^2} + \frac{\sigma_z^2}{\sigma_y^2} \geq \frac{1-(\overline{Z'})^2}{\overline{Z^2}} - 1 \tag{A3.13}$$

The reasoning leading from (A3.3) to (A3.5) shows that

$$\frac{\sigma_z^2}{\sigma_x^2} + \frac{\sigma_z^2}{\sigma_y^2} \geq \mathrm{Tan}^2\left(\frac{\pi}{2} - \frac{\phi}{2}\right) \tag{A3.14}$$

Q.E.D.

APPENDIX IV

The following notes are helpful in interpreting the sequence of steps leading from Equation (11.27) to Equations (11.33), (11.34) in Section XI.

In these notes the term "end point constellation" is used to denote a constellation for which the points $P_1, P_2 \ldots P_N$ are restricted to the center and the extreme ends of a sector S as shown in Figure A4.1.

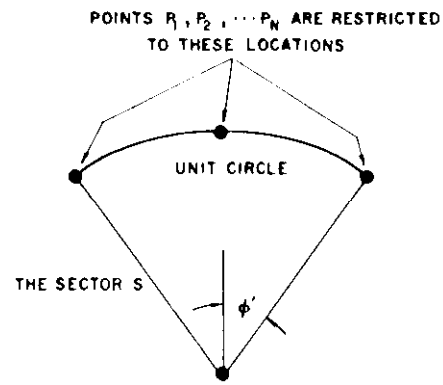

Figure A4.1

Notes

1. In effect (11.26) asserts that there exists an end point constellation $C_1(\phi')$ that has the same values of Y', $\overline{X^2}$ and $\overline{Y^2}$ as C and which (consequently) produces the same value of σ^2 as C. Equation (11.27) asserts that $C_1(\phi')$(normally) is confined to a sector S with a half angle ϕ' smaller than ϕ.

2. In effect (11.30) says that since C produces the same value of σ^2 as one end point constellation for S [namely $C_1(\phi')$], it must produce a value of σ^2 that is greater than (or equal to) that for the "best" endpoint constellation $C_2(\phi')$ for S. The right hand member of (11.31) is the "best" value of σ^2 for end point constellations in S.

3. The step involved in (11.32) amounts to saying that since σ^2 is greater than (or equal to) that for the best end point constellation $C_2(\phi')$ available from the sector S, it must be greater than (or equal to) σ^2 for the "best" end point constellation when all angles in the inverval $0 \leq \phi' \leq \phi$ are considered. The right hand member of (11.33 and 11.34)

is the best value of σ^2 for end point constellations available in the interval $0 \leq \phi' \leq \phi$.

4. A graph of the function

$$F = \frac{1}{4 \cos \frac{\phi}{2} \sin^2 \frac{\phi}{2}}$$

is shown in Figure A4.2. The lower bound (11.34) is a consequence of the fact that the curve turns upward at $\phi = 2\pi/3$.

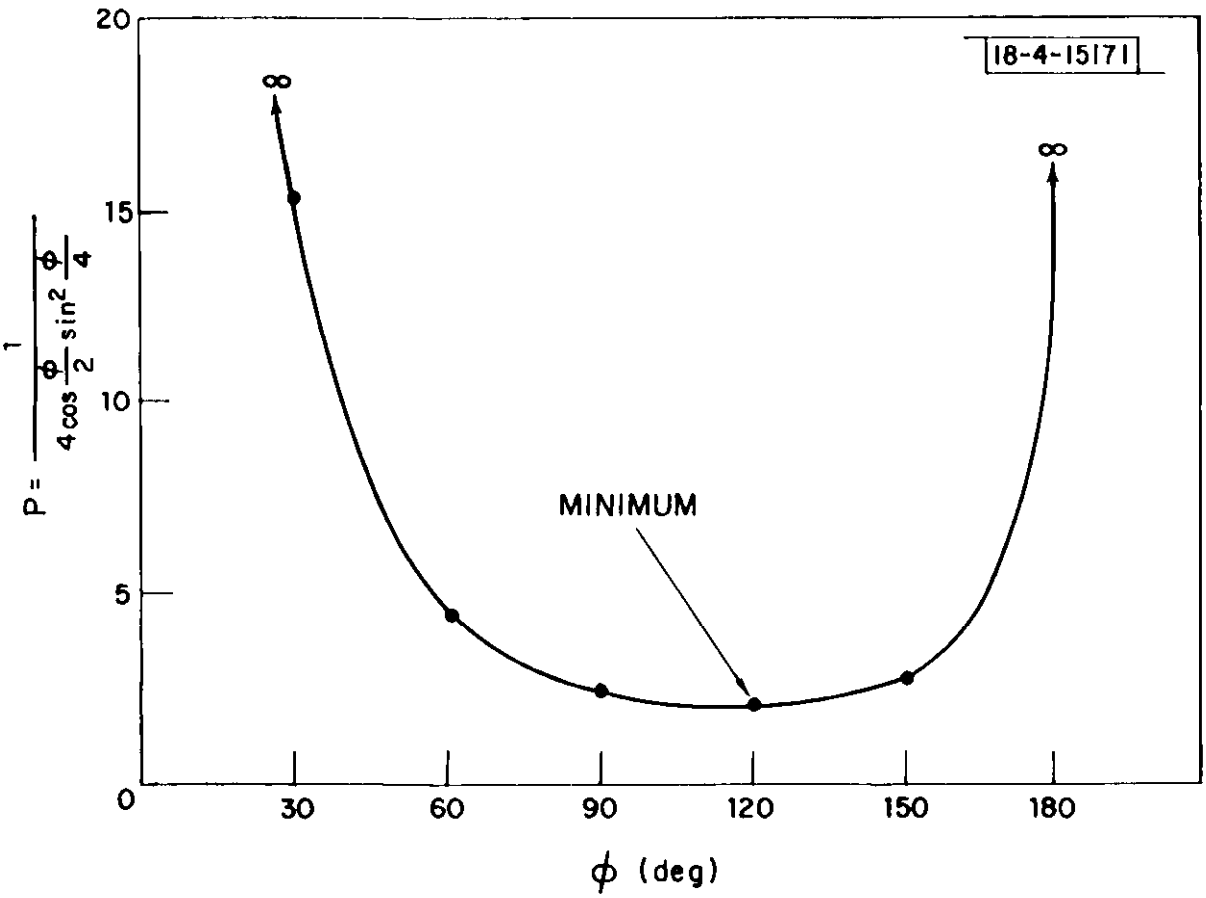
18-4-15171
$P = \frac{1}{\frac{\phi}{4\cos\frac{\phi}{2}\sin^2\frac{\phi}{4}}}$
20
15
10
5
0
∞
∞
MINIMUM
30
60
90
120
150
180
ϕ (deg)

Figure A4.2